JIRRS
Journal International Review of Research Studies

Received: 02/05/2026 - **Accepted:** 25/06/2026
Vol: 01.09
DOI: 10.66104/x7rh8151
Pages: 1-39

QUANTIFICATION OF $BACL_2$-REMOBILIZABLE NICKEL IN ATMOSPHERIC SULFURIC LEACHING RESIDUES FROM FERRUGINOUS NICKEL ORES USING BARIUM CHLORIDE AS A SULFATE PROBE

Antonio Clareti Pereira, PhD
PhD in Chemical Engineering
University of São Paulo (USP)
Belo Horizonte, Minas Gerais, Brazil
E-mail: claretipereira@gmail.com
ORCID: https://orcid.org/0000-0001-8115-4279

Abstract

Nickel losses during atmospheric sulfuric acid leaching are commonly attributed to incomplete dissolution of nickel-bearing minerals; however, secondary retention phenomena associated with sulfate-bearing and iron-rich phases may also contribute to nickel remaining in leach residues. This study evaluated an operational diagnostic procedure that quantifies the $BaCl_2$-remobilizable nickel fraction by adding barium chloride to atmospheric sulfuric leaching residues generated from a ferruginous nickel ore containing 1.00 wt.% Ni. Five residues from previous leaching tests were treated using 150 g of residue, approximately 1341 g of water, and 7.84-9.27 g of $BaCl_2$ at 70-80 °C under acidic conditions. Total contact time was 240 min, and the final kinetic sample reported in this manuscript corresponds to 210 min. The leaching residues initially contained 0.616-0.728 wt.% Ni. Following $BaCl_2$ treatment, measurable quantities of nickel were released to solution, corresponding to operationally defined remobilized fractions of 0.75-6.48% of the initial nickel inventory present in the residues, with an average of 3.67%. Final reported dissolved nickel concentrations ranged from 7.64 to 60.56 mg L^{-1}. These results indicate that a limited but measurable portion of residual nickel is susceptible to remobilization under sulfate-scavenging conditions. Because no independent sulfate measurements, replicate extractions, control tests, or post-treatment solid-phase mineralogical characterization were available for the historical residue set, the method is interpreted as an operational extraction test rather than direct mineralogical proof of nickel co-precipitation. Thermodynamic calculations support the plausibility of $BaSO_4$ formation as a strong sulfate sink, but they are treated as standard-state screening calculations and not as full activity-corrected aqueous speciation modeling. The method therefore provides a practical diagnostic approach for estimating $BaCl_2$-remobilizable nickel and for guiding future validation of sulfate-related nickel retention mechanisms in atmospheric sulfuric acid leaching circuits.

Keywords: nickel; atmospheric leaching; $BaCl_2$-remobilizable fraction; barium chloride; sulfate scavenging; laterite; diagnostic extraction; hydrometallurgy.

1. Introduction

JIRRS
Journal International Review of Research Studies
Received: 02/05/2026 - **Accepted:** 25/06/2026
Vol: 01.09
DOI: 10.66104/x7rh8151
Pages: 1-39

Nickel laterite ores have become increasingly important for supplying nickel to the battery, stainless steel, and energy transition sectors. The growing demand for nickel has intensified interest in developing more efficient and sustainable processing routes for lateritic resources, particularly because laterites constitute a large fraction of the global nickel resource base (Pell et al., 2021; Golroudbary et al., 2023; Soh Tamehe et al., 2024). However, the treatment of lateritic ores remains technically challenging due to their complex mineralogy, variable weathering profiles, and heterogeneous distribution of nickel among iron oxyhydroxides, phyllosilicates, poorly crystalline Fe–Si phases, and secondary alteration products.

Hydrometallurgical processing of nickel laterites is commonly based on atmospheric acid leaching or high-pressure acid leaching (HPAL), depending on ore mineralogy, nickel deportment, and process objectives. Atmospheric leaching has been widely investigated because of its operational simplicity and lower capital intensity, although nickel recovery depends strongly on acid dosage, temperature, residence time, redox conditions, and mineralogical reactivity (Hosseini Nasab et al., 2020; Astuti et al., 2024; Prameswara et al., 2024; Prasetya et al., 2025; Ribeiro et al., 2025). HPAL, in contrast, is generally more effective for limonitic ores because it promotes extensive dissolution of nickel-bearing iron oxyhydroxides, but it requires high capital investment, high-pressure equipment, and careful management of acid consumption, iron dissolution, and downstream neutralization (Çoban & Baş, 2024; Gharaei et al., 2024; Dickson et al., 2025; Bana et al., 2025; Surya et al., 2026). Recent studies on high-pressure nickel–cobalt systems and hydrometallurgical refinery development further highlight the continuing relevance of pressure leaching and downstream purification in modern nickel flowsheets (Chen et al., 2026; Marte & Boone, 2025).

In addition to conventional atmospheric leaching and HPAL, alternative and hybrid routes have been investigated to improve nickel and cobalt recovery from lateritic resources. These include bioleaching approaches for low-grade laterites, combined hydrometallurgical processes, selective sulfuric acid leaching strategies, and integrated recovery flowsheets designed to improve selectivity and reduce waste generation (Ester et al., 2020; Abdollahi et al., 2024; Caetano et al., 2024; Li et al., 2023; Zablotskaya et al., 2025). Studies on reduced ferriferous laterites and oxidized nickel ores have also shown that sulfuric acid leaching performance depends not only on acid availability, but also on the mineralogical form of nickel

JIRRS
Journal International Review of Research Studies
Received: 02/05/2026 - **Accepted:** 25/06/2026
Vol: 01.09
DOI: 10.66104/x7rh8151
Pages: 1-39

and cobalt and on the selectivity of dissolution relative to iron and other gangue elements (Zablotskaya et al., 2022; Zablotskaya et al., 2023).

The metallurgical response of nickel laterites is strongly controlled by mineralogy. Nickel may occur as a substituent in goethite, as a component of serpentine- or vermiculite-type phyllosilicates, or in poorly crystalline ferruginous silicate domains. These mineral hosts differ in chemical stability and reactivity during acid leaching, which affects nickel extraction kinetics, acid consumption, and residue composition. For this reason, modern geometallurgical approaches emphasize the need to relate mineralogical deportment, particle texture, and process response rather than relying only on bulk chemical composition (Dehaine et al., 2021; Butcher et al., 2023). Previous studies have shown that lateritic ores with similar nickel grades may exhibit different metallurgical behavior because nickel deportment and mineral associations vary substantially within and between deposits (Dybowska et al., 2022; Jeong et al., 2025; Araujo et al., 2026).

Despite the large number of studies on nickel laterite leaching, many investigations still treat the ore or residue as a bulk material and focus primarily on overall extraction values. In such cases, the residual nickel remaining after leaching is often reported as a single value, without distinguishing among chemically labile, adsorbed, occluded, sulfate-associated, or refractory mineral-bound nickel forms. This limitation is particularly important because residual nickel may occur in several forms with different chemical stability and different implications for process diagnosis. Several studies have optimized acid leaching conditions using bulk extraction indicators, but the mechanistic nature of the residual nickel inventory is not always elucidated (Top et al., 2020; Li et al., 2020; Yunita & Mubarok, 2021; Komnitsas et al., 2026; Ni'mah et al., 2026).

The residues studied in the present work originated from previous atmospheric sulfuric acid leaching tests performed on a ferruginous nickel laterite ore containing approximately 1.0 wt.% Ni. Residual nickel contents ranged from 0.616 to 0.728 wt.%, indicating that a substantial nickel inventory remained in the solid phase after primary leaching. This residual nickel may occur in refractory primary minerals, iron oxyhydroxides, adsorbed surface species, secondary sulfate-bearing phases, entrained pore solution, or combinations of these forms. Therefore, the residual nickel inventory should be interpreted as a heterogeneous pool with different chemical stabilities rather than as a single mineralogical phase.

JIRRS
Journal International Review of Research Studies
Received: 02/05/2026 - **Accepted:** 25/06/2026
Vol: 01.09
DOI: 10.66104/x7rh8151
Pages: 1-39

Controlled $BaCl_2$ experiments were used to assess whether a portion of this residual nickel could be remobilized when sulfate is scavenged as highly insoluble $BaSO_4$. In this study, nickel released after $BaCl_2$ addition is interpreted as an operationally defined $BaCl_2$-remobilizable nickel fraction. The test does not identify the specific mineralogical host of nickel and does not quantify total residual nickel, because stable oxide-, silicate-, or refractory mineral-bound nickel may remain unaffected under the diagnostic conditions.

This work aimed not to promote $BaCl_2$ as an industrial nickel-recovery reagent, but to evaluate a diagnostic method for estimating a labile nickel fraction that responds to sulfate scavenging. By combining kinetic observations, solution chemistry, and nickel balance calculations, the method provides an operational indicator of sulfate-related nickel retention that can support metallurgical accounting, process diagnosis, and the identification of targets for future mineralogical validation. The interpretation is based on six connected concepts: sulfuric acid leaching dissolves part of the nickel from ferruginous lateritic material; acid leaching, cooling, filtration, or neutralization may produce Fe–Ni sulfate environments; nickel may be retained by incorporation, adsorption, occlusion, or secondary salt formation; Ba^{2+} addition reduces sulfate activity via $BaSO_4$ precipitation; the released nickel represents an operationally remobilizable fraction; and the method is a comparative diagnostic tool, not definitive mineralogical evidence.

2. Materials and methods

2.1. Feed ore

A bulk sample of limonitic nickel laterite from Northeastern Brazil was used in this study. The material is representative of ferruginous lateritic profiles developed under tropical weathering conditions, in which nickel may be distributed among iron oxyhydroxides, phyllosilicates, and poorly crystalline Fe–Si phases. Similar mineralogical and geochemical features have been described for lateritic systems in Brazil and other tropical nickel laterite provinces (Dybowska et al., 2022; Domènech et al., 2022; Soh Tamehe et al., 2024).

The sample was homogenized and split into representative aliquots for chemical analysis, particle-size separation, mineralogical characterization, and atmospheric leaching experiments. The chemical composition of the feed ore was determined before the leaching tests and is presented in Table 1.

JIRRS
Journal International Review of Research Studies
Received: 02/05/2026 - **Accepted:** 25/06/2026
Vol: 01.09
DOI: 10.66104/x7rh8151
Pages: 1-39

Table 1. Chemical composition of the feed ore

Component	Content (wt.%)
Fe	42.9
Ni	1.00
Mg	1.61
Mn	0.698
Cr	1.08
Al	0.938
Si	7.86
Co	0.053
LOI	10.1

The high iron content indicates the presence of ferruginous minerals typical of limonitic and lateritic nickel ores. Nickel is primarily associated with iron oxyhydroxides and weathering products (Butcher et al., 2023; Dehaine et al., 2021).

2.2. Sulfuric Leaching Residues

Five sulfuric leaching residues from previous tests were examined. As shown in Table 2, residues contained 0.616–0.728 wt.% Ni, with iron as the dominant element (33.8–39.0 wt.% Fe), ndicating that a measurable residual nickel inventory remained in the solid phase after leaching.

Table 2. Chemical composition of the sulfuric leaching residues used in $BaCl_2$ extraction experiments.

Residue	Fe (%)	Ni (%)	Cr (%)	Mg (%)	Mn (%)	Si (%)
E1	37.4	0.641	1.86	0.916	0.297	13.4
E2	39.0	0.724	1.88	0.849	0.312	12.8
E3	38.1	0.728	1.87	0.912	0.325	12.7
E4	37.0	0.688	0.781	0.274	0.270	13.6
E5	33.8	0.616	1.80	0.929	0.285	13.9

Source: Chemical characterization of atmospheric sulfuric leaching residues performed by ICP-OES after alkaline fusion with Na_2CO_3–$Na_2B_4O_7$ flux. Data derived from the author's atmospheric sulfuric leaching research program.

Residual nickel ranged from 0.616 to 0.728 wt.%, indicating much remained after sulfuric acid leaching. The higher iron grade than the feed ore suggests nickel, magnesium, and manganese dissolved more, enriching residual ferruginous phases.

Persistent nickel levels after leaching imply residual nickel could be in refractory minerals, adsorbed on iron surfaces, or retained in pore solutions or secondary sulfates and iron compounds. Without post-treatment mineralogical analysis, these are considered possible mechanisms rather than confirmed hosts (Hosseini Nasab et al., 2020; Santos et al., 2021).

JIRRS
Journal International Review of Research Studies
Received: 02/05/2026 - **Accepted:** 25/06/2026
Vol: 01.09
DOI: 10.66104/x7rh8151
Pages: 1-39

The original feed ore and sulfuric leaching residues (Figure 1) show chemical changes, especially in nickel, iron, magnesium, and manganese. Increased iron and silica proportions, with persistent nickel, indicate preferential dissolution of acid-soluble components and retention of some nickel in residual or secondary forms.

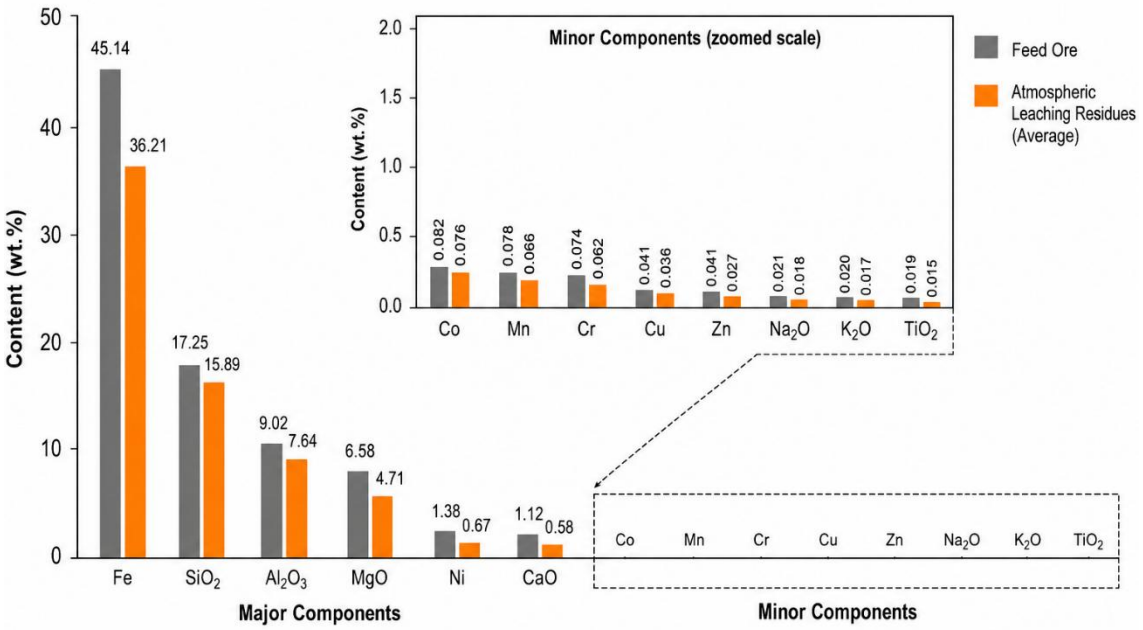


Figure 1. Comparison between the chemical composition of the feed ore and atmospheric leaching residues. Source: Experimental data obtained during this study.

Figure 1 shows that atmospheric sulfuric leaching removed much of the nickel, decreasing it from 1.00 wt.% to 0.616–0.728 wt.%. Nickel depletion was about 27–38%. Iron levels stayed high at 33.8–39.0 wt.%, showing only partial dissolution of iron-bearing phases.

The enrichment of silica in the residues, from 7.86 wt.% in the feed ore to approximately 12.4–13.9 wt.% in the leached solids, reflects the preferential dissolution of acid-soluble phases and the concentration of relatively inert silicate minerals. Likewise, the substantial reductions observed for magnesium, manganese, and cobalt suggest preferential dissolution of these elements during sulfuric acid leaching.

High nickel levels in the residues, despite primary leaching, indicate that the remaining nickel inventory cannot be explained only from solution assays. However, without mineralogical confirmation, the specific nickel hosts remain unresolved; the $BaCl_2$ test should therefore be used as a diagnostic probe of remobilizability rather than as proof of a single co-precipitation mechanism.

The residues E1-E5 were obtained from previous atmospheric sulfuric acid leaching experiments. The available archival information is sufficient to define the residue chemistry

JIRRS
Journal International Review of Research Studies
Received: 02/05/2026 - **Accepted:** 25/06/2026
Vol: 01.09
DOI: 10.66104/x7rh8151
Pages: 1-39

and the $BaCl_2$ diagnostic conditions, but not all original leaching variables were recorded for each residue. Table 3 summarizes the information available for interpretation and the variables that must be documented in future validation campaigns.

Table 3. Source-campaign information available for residues E1-E5 and reproducibility boundaries.

Information item	Available information for E1-E5	Status in this study	Implication for interpretation
Feed and residue identity	Ferruginous nickel ore with 1.00 wt.% Ni; residues E1-E5 after atmospheric sulfuric acid leaching	Available	Defines the experimental material and residue set
Residue chemistry	Ni = 0.616-0.728 wt.%; Fe = 33.8-39.0 wt.%	Available	Supports comparison of remobilized nickel among residues
$BaCl_2$ diagnostic conditions	150 g residue; 1341.5 g water; 7.84-9.27 g $BaCl_2$; 70-80 °C; pH 1.3-2.0; 250 rpm; 240 min total contact; final reported kinetic sample at 210 min	Available	Defines the operational extraction window
Original leaching variables	Acid concentration, pulp density, redox potential, sulfate concentration, and detailed time-temperature history for each source leach were not available in the archival dataset	Not fully available	Limits external validity and prevents mechanistic attribution solely from residue-to-residue variability
Filtration/washing history	Residues were acid-washed with process water from the original circuit before $BaCl_2$ treatment	Partially available	Reduces, but does not fully eliminate, possible pore-solution effects

2.3. Residue Preparation

Before $BaCl_2$ treatment, atmospheric sulfuric leaching residues underwent acidic washing with process water from the original circuit to remove pore solutions containing nickel sulfate and maintain acidic conditions, thereby minimizing iron hydrolysis.

The washing stage aimed to remove dissolved nickel from liquors while keeping nickel in solid phases. Nickel released during $BaCl_2$ treatment was primarily derived from solid species, not from pore solutions. After washing, residues were filtered and directly extracted with $BaCl_2$ without pH adjustments.

The overall experimental methodology used in this study is summarized in Figure 2.

JIRRS
Journal International Review of Research Studies
Received: 02/05/2026 - **Accepted:** 25/06/2026
Vol: 01.09
DOI: 10.66104/x7rh8151
Pages: 1-39

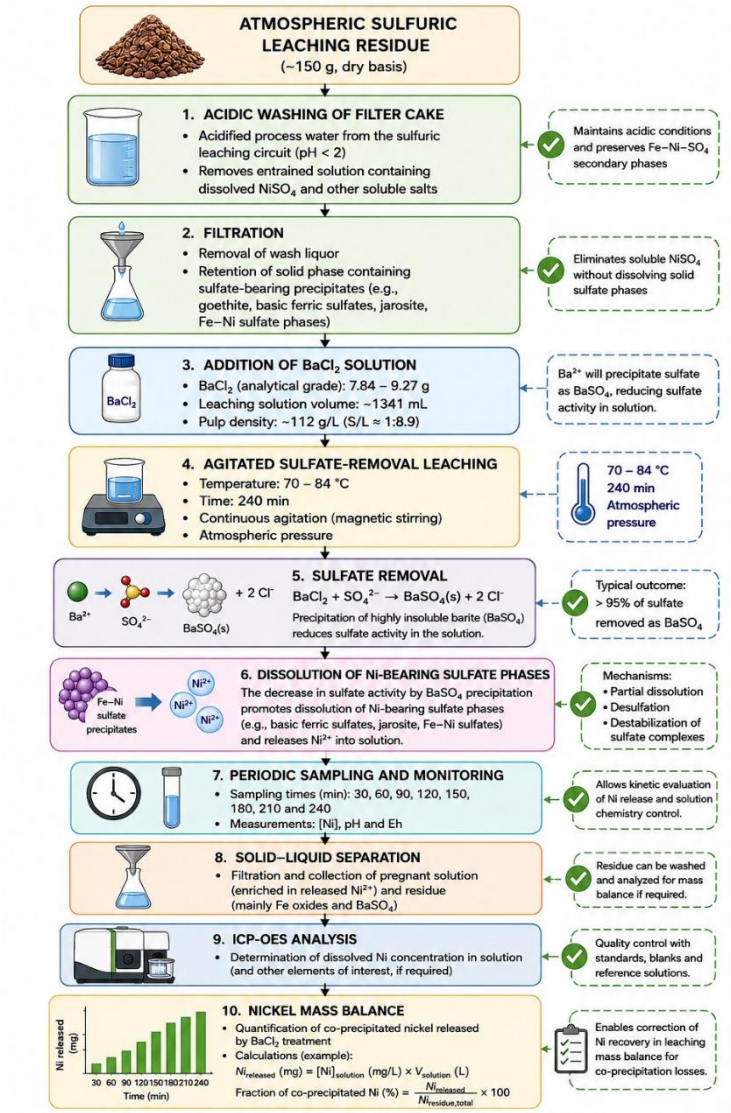


Figure 2. Experimental flow sheet adopted for preparation of residues and quantification of $BaCl_2$-remobilizable nickel. Source: Authors (2026).

As shown in Figure 2, the methodology consisted of four sequential stages: (i) preparation of washed acidic residues to reduce entrained nickel-bearing solutions, (ii) sulfate scavenging through $BaSO_4$ precipitation after $BaCl_2$ addition, (iii) remobilization of nickel that is labile under the imposed sulfate-scavenging conditions, and (iv) quantification of dissolved nickel by solution analysis and operational mass-balance calculations.

The diagnostic principle of the method is based on the very low solubility of barium sulfate. When Ba^{2+} is added to the acidic residue suspension, sulfate may be removed from solution through $BaSO_4$ precipitation. This reduction in sulfate activity may shift dissolution equilibria involving sulfate-associated nickel species and promote the release of a labile nickel fraction into solution. In the present study, this mechanism is considered chemically plausible

JIRRS
Journal International Review of Research Studies
Received: 02/05/2026 - **Accepted:** 25/06/2026
Vol: 01.09
DOI: 10.66104/x7rh8151
Pages: 1-39

but operational, because sulfate concentrations before and after $BaCl_2$ addition, residual dissolved Ba^{2+}, and post-treatment solid-phase speciation were not directly measured.

Therefore, the method does not quantify total nickel retained in the residue by all possible mechanisms. Instead, it estimates the $BaCl_2$-remobilizable nickel fraction under the selected acidic and sulfate-scavenging conditions, allowing comparison of nickel remobilization behavior among the investigated residues. Because iron-rich hydrometallurgical residues may contain poorly crystalline ferric hydroxides, goethite-like phases, jarosite-type compounds, or mixed sulfate-bearing environments, nickel remobilization under $BaCl_2$ treatment should be interpreted as an operational response rather than as direct mineralogical proof of a single nickel host phase (Niu et al., 2021; Xing et al., 2024; Yang et al., 2025; Zhu et al., 2025).

2.4. $BaCl_2$ extraction procedure

Approximately 150 g of residue were treated with aqueous barium chloride solutions under atmospheric pressure. Barium chloride was added in excess relative to sulfate estimated from previous leaching records; however, because sulfate was not measured before and after $BaCl_2$ addition in the present dataset, this stoichiometric basis is reported as an experimental estimate rather than as an independently closed sulfate balance.

Following preparation of the washed atmospheric leaching residues, $BaCl_2$ treatment tests were conducted to investigate the remobilization of nickel under sulfate-scavenging conditions. The experimental conditions were selected to maintain acidity while promoting sulfate removal via barium sulfate precipitation. Table 4 summarizes the principal operating parameters employed in all experiments.

Table 4. Experimental conditions adopted in the $BaCl_2$ treatment tests. Source: Experimental records from atmospheric sulfuric leaching tests previously conducted by the author.

Parameter	Value
Residue mass	150 g
Water mass	1341.5 g
$BaCl_2$ addition	7.84–9.27 g
Temperature	70–80°C
pH range	1.3–2.0
Agitation	250 rpm
Residence time	240 min

Source: Experimental data obtained during the atmospheric sulfuric leaching residue characterization and subsequent $BaCl_2$ extraction program conducted by the authors.

JIRRS
Journal International Review of Research Studies
Received: 02/05/2026 - **Accepted:** 25/06/2026
Vol: 01.09
DOI: 10.66104/x7rh8151
Pages: 1-39

The operating conditions aimed to maximize contact between residue particles and $BaCl_2$ solution in an acid environment from sulfuric leaching. The prior acidic wash removed nickel sulfate liquor from filter cake pores, ensuring the nickel measured mainly came from nickel associated with sulfate-bearing secondary phases in the residue.

Temperatures of 70-80 °C promote reaction progress and maintain acidity. Barium ions react with sulfate to form insoluble $BaSO_4$, reducing sulfate activity. Since no controls with acidified water, chloride-only, calcium chloride, or a residue without $BaCl_2$ were performed, nickel release is interpreted as an operational response to $BaCl_2$, rather than a specific mechanism.

The relatively narrow range of $BaCl_2$ dosages (7.84-9.27 g per 150 g residue) was selected to provide a practical excess for sulfate scavenging while minimizing unnecessary reagent use. The resulting nickel concentrations measured in the pregnant liquors were subsequently used to establish an operational nickel release balance and to estimate the magnitude of the $BaCl_2$-remobilizable nickel fraction.

The experimental method aimed to measure nickel remobilized during sulfate scavenging while minimizing artifacts from secondary hydrolysis. A lab-scale system with temperature control, reflux, agitation, and sampling maintained consistent conditions over 240 min (see Figure 3). Kinetic samples were collected up to 210 min, and the concentration at this duration is reported.

JIRRS
Journal International Review of Research Studies
Received: 02/05/2026 - **Accepted:** 25/06/2026
Vol: 01.09
DOI: 10.66104/x7rh8151
Pages: 1-39

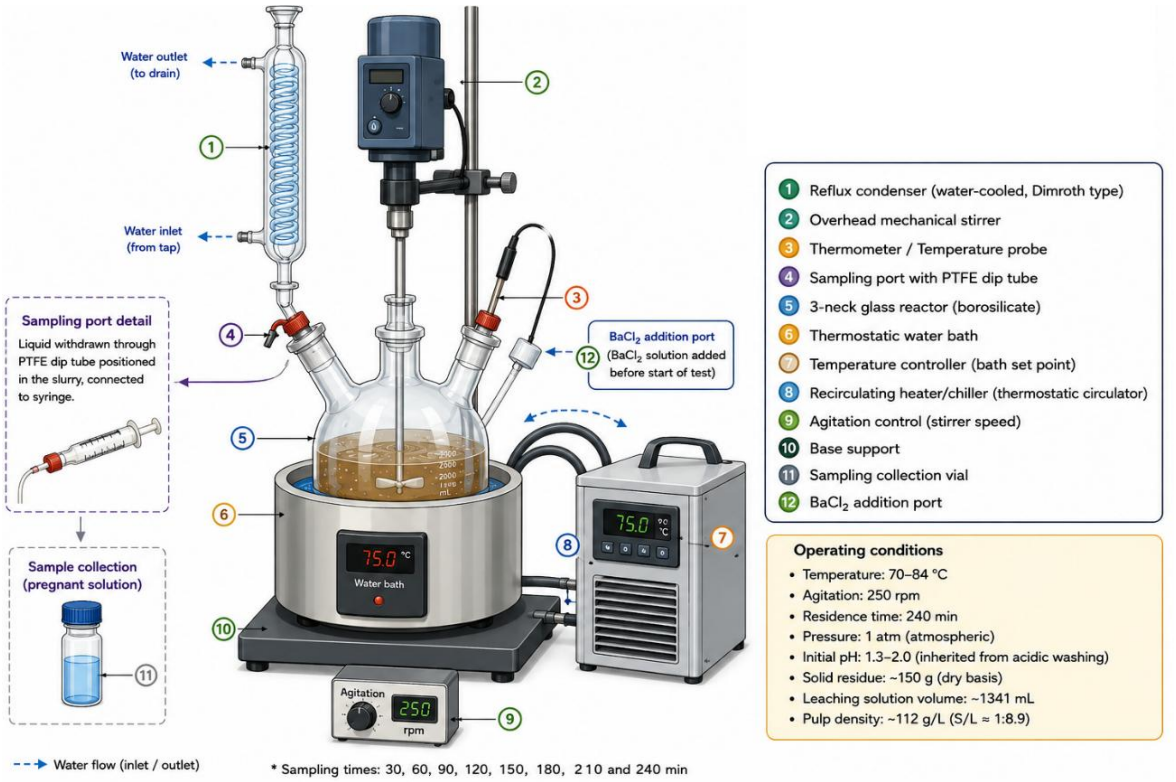


Figure 3. Schematic representation of the $BaCl_2$ extraction apparatus, including reflux condenser, agitation system, temperature control and sampling ports.

The extraction system consisted of a borosilicate glass reactor equipped with an overhead mechanical stirrer, a water-cooled reflux condenser, a temperature probe, and a sampling port. Heating was provided by an electric mantle coupled to a temperature controller, maintaining the slurry between 70 and 80 °C throughout the experiments. Samples of the pregnant solution were periodically withdrawn at 30-min intervals up to 210 min for nickel determination by ICP-OES, while the overall contact time was maintained at 240 min before final filtration and washing. (Laubertová et al., 2024)

The use of a reflux condenser minimized water losses and helped maintain approximately constant solution volume during the tests. Because the residues originated from acidic washing stages after sulfuric leaching, the filter cakes remained acidic before $BaCl_2$ treatment. No additional acidification was applied, which reduced the risk of adding a separate acid-leaching effect; nevertheless, the absence of acidified-water and chloride-only controls means that alternative release mechanisms cannot be fully excluded.

The apparatus was designed to reproduce controlled acidic, heated, and agitated diagnostic conditions while allowing quantitative monitoring of nickel released to solution. The configuration provides information on $BaCl_2$-remobilizable nickel, but it does not by itself

JIRRS
Journal International Review of Research Studies
Received: 02/05/2026 - **Accepted:** 25/06/2026
Vol: 01.09
DOI: 10.66104/x7rh8151
Pages: 1-39

identify the solid host phase or prove that $BaCl_2$ would be suitable as an industrial recovery reagent.

No additional control experiments were available for the historical residue set used in this manuscript. Accordingly, the present revision explicitly frames the method as an operational diagnostic extraction and identifies the controls required for future validation. These controls are summarized in Table 5.

Table 5. Recommended validation controls and measurements for future $BaCl_2$ diagnostic campaigns.

Control or measurement	Purpose	Status in present study	Interpretive consequence
Acidified-water control	Separate acid/temperature desorption from sulfate scavenging	Not performed	Alternative acidic desorption cannot be fully excluded
NaCl or $CaCl_2$ ionic-strength control	Separate chloride/ionic-strength effects from Ba^{2+} sulfate scavenging	Not performed	Chloride and ionic-strength effects remain possible contributors
$BaCl_2$ blank without residue	Check reagent contamination and background nickel	Reagent blanks available for analytical work; dedicated $BaCl_2$ blank not reported	Blank contribution considered low but not fully isolated for this test
Residue treated without $BaCl_2$	Evaluate continued leaching under identical temperature and pH	Not performed	Continued dissolution cannot be quantified separately
Replicate $BaCl_2$ extractions	Estimate reproducibility and propagated uncertainty	Not performed	Residue-to-residue variability is interpreted as exploratory
Sulfate before/after $BaCl_2$ and residual Ba^{2+}	Confirm sulfate removal and non-limiting barium availability	Not measured	Sulfate scavenging remains thermodynamically supported but not analytically closed
XRD/SEM-EDS/FTIR or sequential extraction	Identify nickel-hosting phases and $BaSO_4$ formation in solids	Not performed	Mineralogical hosts remain unconfirmed

2.5. Analytical Procedures

Solid samples were chemically characterized using complementary analytical procedures to quantify major and minor elements in the atmospheric leaching residues.

Major elements (Al, Fe, Mg, Mn, Ni, Cr, Si, and Co) were determined after alkaline fusion using a sodium carbonate (Na_2CO_3) and sodium tetraborate ($Na_2B_4O_7$) flux mixture,

JIRRS
Journal International Review of Research Studies
Received: 02/05/2026 - **Accepted:** 25/06/2026
Vol: 01.09
DOI: 10.66104/x7rh8151
Pages: 1-39

followed by dissolution of the fused bead and elemental determination by inductively coupled plasma optical emission spectrometry (ICP-OES). This approach ensured complete decomposition of silicate and oxide phases commonly present in ferruginous lateritic materials.

Copper concentrations were determined after aqua regia digestion followed by ICP-OES analysis. Loss on ignition (LOI) was measured gravimetrically after calcination at 1000 °C for 2 h in a laboratory muffle furnace.

Liquid samples collected during $BaCl_2$ extraction tests and washing stages were filtered, acid-stabilized when needed, and analyzed by ICP-OES. Nickel concentrations were reported in μg mL^{-1} and converted into dissolved nickel masses using measured solution volumes.

Periodic solution sampling at 210 min enabled evaluation of nickel dissolution kinetics, while maintaining total contact for 240 min before final filtration and washing. All final kinetic concentrations reported in the Results correspond to the 210 min liquor sample.

2.6. Quality Assurance and Quality Control (QA/QC)

A QA/QC program was implemented to support reliable analytical data for nickel balance calculations, including certified reference materials, analytical standards, and reagent blanks. The QA/QC program supports the quality of chemical determinations, but it does not replace replicate extraction tests or propagated uncertainty estimates for the $BaCl_2$ diagnostic procedure.

The reference materials employed were:

• VRM-04 (multi-element certified reference material);

• IGS23 (certified copper standard).

The performance of principal quality control standards is summarized in Table 6.

Table 6. Quality control results obtained for certified reference materials and analytical standards used in the study. Source: Analytical quality control data obtained during the experimental program using certified reference material VRM-04 and analytical standard IGS23.

Element	Result	Certified Range
Ni	4.14	3.928–4.340
Fe	7.83	7.457–8.237
Al	7.53	7.046–7.786
Mg	10.7	10.1–11.16
Cu	0.012	0.010–0.016

Source: Analytical quality control data obtained from certified reference material (VRM-04) and certified analytical standard (IGS23) analyzed during the QA/QC program of the present study.

The analytical results for all certified materials were within their acceptance intervals, confirming the accuracy and precision of the procedures. Nickel, the primary element studied,

JIRRS
Journal International Review of Research Studies
Received: 02/05/2026 - **Accepted:** 25/06/2026
Vol: 01.09
DOI: 10.66104/x7rh8151
Pages: 1-39

had a measured value of 4.14 wt.%, which matched the certified range. Similar agreement was seen for iron, aluminum, magnesium, and copper.

Reagent blanks were analyzed alongside certified standards to assess contamination from sample prep, fusion, digestion, or analysis. Results shown in Table 7.

Table 7. Results obtained for analytical blank samples used during the quality control program. Source: Analytical blank determinations performed during the quality assurance and quality control program of the experimental campaign.

Element	Blank Result
Ni	<0.178%
Fe	<0.369%
Mg	<0.169%
Mn	<0.053%
Al	<0.074%

All monitored elements were below their quantification limits. The absence of detectable nickel in the blanks confirms that the nickel in the liquors came only from the tested residues, not contamination.

Results from reference materials and blanks support confidence in the reported nickel concentrations. However, because duplicate or triplicate $BaCl_2$ extraction tests were not performed, the variability discussed in this study should be interpreted primarily as between-residue variability rather than as an operational estimate of experimental reproducibility.

2.7. Nickel Mass Balance Methodology

This work aimed to quantify the nickel remobilized during $BaCl_2$ sulfate-based scavenging from sulfuric acid leaching residues. These values are operational results and not total $BaCl_2$-remobilizable nickel or mineralogical speciation.

Nickel remobilization was evaluated using a solution-phase balance involving three terms:

1. Nickel initially present in the residue;
2. Nickel dissolved in the $BaCl_2$ pregnant solution;
3. Nickel recovered during the washing stage.

The initial nickel inventory in each residue was calculated from:

$$Ni_{initial} = M_{residue} \times Ni(\%) / 100 \quad \text{.....Equation 1}$$

where $M_{residue}$ is the dry residue mass (g), and Ni(%) is the nickel concentration determined by ICP-OES.

JIRRS
Journal International Review of Research Studies
Received: 02/05/2026 - **Accepted:** 25/06/2026
Vol: 01.09
DOI: 10.66104/x7rh8151
Pages: 1-39

The dissolved nickel mass in each pregnant liquor was calculated from:

$$Ni_{liquor} = C_{Ni} \times V_{liquor} \ldots\ldots\ldots \text{Equation 2}$$

where C_{Ni} is the nickel concentration (mg L^{-1}), and V_{liquor} is the measured liquor volume (L).

Similarly, nickel recovered during the washing stage was calculated from:

$$Ni_{wash} = C_{wash} \times V_{wash} \ldots\ldots\ldots \text{Equation 3}$$

The total remobilized nickel was obtained from:

$$Ni_{total} = Ni_{liquor} + Ni_{wash} \ldots\ldots\ldots \text{Equation 4}$$

The remobilized fraction was calculated as:

$$\text{Recovery (\%)} = (Ni_{total} / Ni_{initial}) \times 100 \ldots\ldots\ldots \text{Equation 5}$$

Because residues were acid-washed immediately after sulfuric leaching, the filter cakes stayed acidic before $BaCl_2$ extraction. This aimed to reduce entrained nickel sulfate liquor and prevent premature ferric hydrolysis during storage and handling. However, pore-solution retention cannot be completely ruled out without specific controls and sulfate measurements.

No initial hydrochloric acid was added. Under these conditions, the nickel recovered during $BaCl_2$ treatment is interpreted as nickel remobilized during the diagnostic extraction. The wording was revised from direct proof of co-precipitation to an operational estimate of a $BaCl_2$-remobilizable fraction.

The calculated nickel recoveries therefore represent an operational estimate of the fraction of the initial residue nickel inventory released to solution under $BaCl_2$ treatment. Direct post-treatment solid nickel analyses were unavailable; consequently, complete mass-balance closure through independent analysis of all solid and liquid streams was not demonstrated.

3. Results and Discussion

3.1. Nickel Dissolution Kinetics During $BaCl_2$ Treatment

Liquor samples during $BaCl_2$ treatment showed nickel release from all residues. This behavior is consistent with sulfate scavenging by $BaSO_4$ precipitation; however, alternative mechanisms cannot be excluded without control tests. Results are in Table 8.

Table 8. Nickel concentrations in intermediate liquors during $BaCl_2$ treatment (µg mL^{-1})

Time (min)	Test 1	Test 2	Test 3	Test 4	Test 5
30	5.52	27.19	45.09	30.16	57.58
60	6.47	28.35	46.54	29.82	57.49
90	6.63	28.18	48.74	29.03	58.32
120	7.36	31.63	46.99	31.22	59.91
150	7.17	31.61	48.68	31.55	59.23
180	7.24	30.30	48.91	31.47	59.94

JIRRS
Journal International Review of Research Studies
Received: 02/05/2026 - **Accepted:** 25/06/2026
Vol: 01.09
DOI: 10.66104/x7rh8151
Pages: 1-39

210	7.64	31.23	51.27	31.72	60.56

Source: Experimental ICP-OES analyses of intermediate liquors collected during $BaCl_2$ treatment of atmospheric sulfuric leaching residues.

The dissolution profiles show that nickel release was initially rapid, with a significant portion reaching the final concentration within 30–60 min, after which it gradually approached equilibrium.

This rapid initial release followed by a slower approach to a plateau is consistent with the presence of a labile nickel fraction superimposed on more stable residual nickel hosts, as observed in studies dealing with nickel loss, impurity removal, and precipitation reactions in hydrometallurgical leachates (Lin & Pan, 2024; Liu et al., 2025; Liu et al., 2022).

To evaluate nickel remobilization kinetics during treatment, nickel levels were monitored during $BaCl_2$ addition. Sampling the liquor allowed the determination of the nickel dissolution rate. The profiles for five residues are shown in Figure 4.

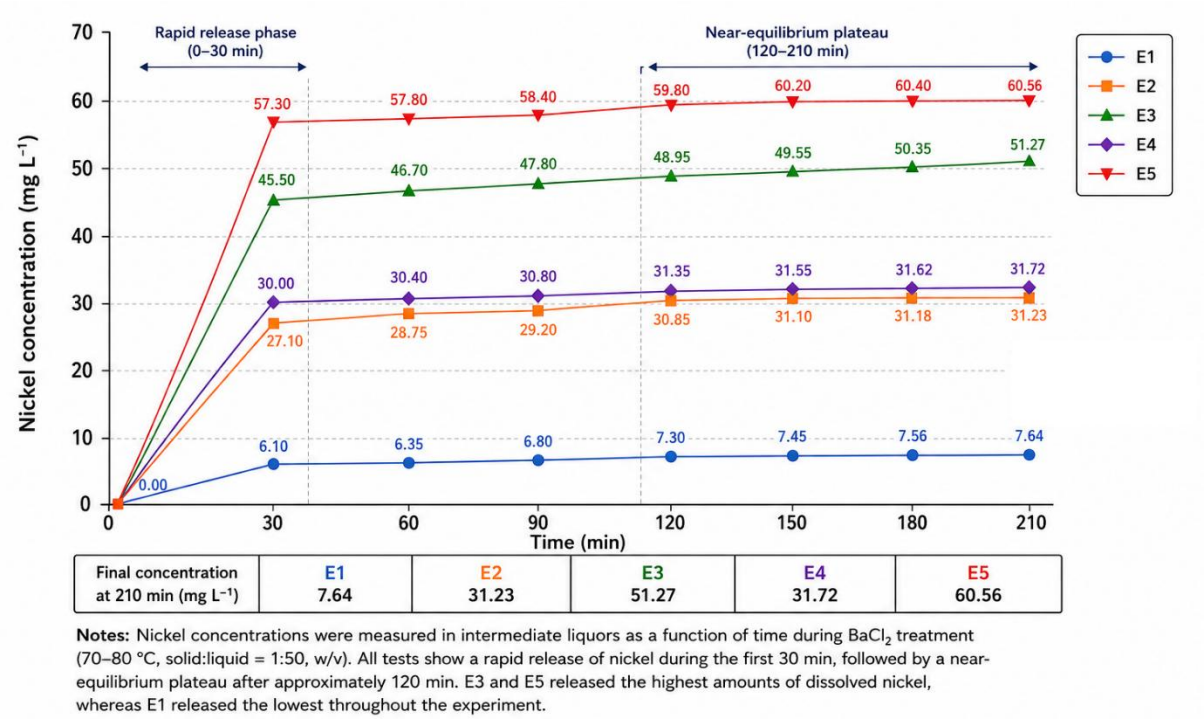


Figure 4. Nickel dissolution kinetics during $BaCl_2$ treatment. Source: Prepared by the authors from ICP-OES analyses of intermediate liquor samples collected during $BaCl_2$ treatment of atmospheric sulfuric leaching residues

Figure 4 demonstrates that nickel release occurred rapidly during the early stages of treatment. In all experiments, a substantial fraction of the final dissolved nickel concentration was reached within the first 30 to 60 min, indicating rapid release from a labile nickel pool once Ba^{2+} ions became available in solution. After this initial stage, nickel concentrations

JIRRS
Journal International Review of Research Studies
Received: 02/05/2026 - **Accepted:** 25/06/2026
Vol: 01.09
DOI: 10.66104/x7rh8151
Pages: 1-39

increased more gradually and approached a near-equilibrium plateau between approximately 120 and 180 min.

The observed kinetic behavior is consistent with the proposed sulfate-scavenging mechanism. As $BaCl_2$ dissociates, dissolved Ba^{2+} ions may react with sulfate species to form highly insoluble $BaSO_4$. Sulfate removal can lower sulfate activity and shift equilibria involving labile sulfate-associated nickel toward release of Ni^{2+}. This interpretation is chemically plausible, but it remains operational because sulfate speciation and solid hosts were not directly measured.

Significant differences were observed among the investigated residues. Test 5 exhibited the highest dissolved nickel concentrations throughout the experiment, reaching approximately 60.6 µg mL^{-1} after 210 min, followed by Test 3 with approximately 51.3 µg mL^{-1}. In contrast, Test 1 remained below 8 µg mL^{-1} during the entire treatment period. These differences indicate that the $BaCl_2$-remobilizable nickel fraction varied considerably among residues.

The attainment of near-constant nickel concentrations after approximately 150 min suggests that most of the $BaCl_2$-remobilizable nickel had already been released into solution under the experimental conditions employed. The remaining nickel inventory persisted in the solid residue after treatment, indicating that a substantial fraction of the residual nickel was associated with phases that were not significantly affected by sulfate scavenging during $BaCl_2$ treatment. Consequently, the results indicate that only a portion of the residual nickel inventory was susceptible to remobilization through the mechanism investigated in this study.

3.2. Nickel Distribution Between Pregnant Liquors and Wash Waters

Nickel concentrations measured in the final washing waters are presented in Table 9

Table 9. Nickel concentrations measured in final wash water

Test	Nickel Concentration (µg mL^{-1})
E1	1.12
E2	3.29
E3	3.25
E4	2.79
E5	3.31
Average	2.75
Standard deviation	0.98
Coefficient of variation (%)	35.6

Source: ICP-OES analyses of wash-water samples collected after filtration and washing of $BaCl_2$-treated atmospheric sulfuric leaching residues.

Nickel was detected in all wash-water streams collected after filtration of the $BaCl_2$-treated residues. The measured concentrations ranged from 1.12 to 3.31 µg mL^{-1}, with an

JIRRS
Journal International Review of Research Studies
Received: 02/05/2026 - **Accepted:** 25/06/2026
Vol: 01.09
DOI: 10.66104/x7rh8151
Pages: 1-39

average value of 2.75 µg mL^{-1}. Although these values were substantially lower than those measured in the corresponding pregnant liquors, they represent an important contribution to the operational nickel release balance.

The presence of nickel in the wash waters indicates that part of the dissolved nickel remained entrained in the pore solution retained by the filter cake after solid–liquid separation. Therefore, excluding the wash-water contribution would lead to an underestimation of the $BaCl_2$-remobilized nickel fraction. The highest wash-water nickel concentrations were observed in Tests 2, 3, and 5, which also showed the highest dissolved nickel concentrations in the pregnant liquors. This consistency suggests that both streams were associated with the same dissolved nickel pool generated during the diagnostic treatment.

Because no residue-without-$BaCl_2$ control was performed, continued dissolution during washing might contribute slightly. Therefore, both the pregnant liquor and wash-water streams were included in the nickel balance to better estimate nickel release during $BaCl_2$ treatment. Nickel concentrations in these streams are shown in Figure 5.

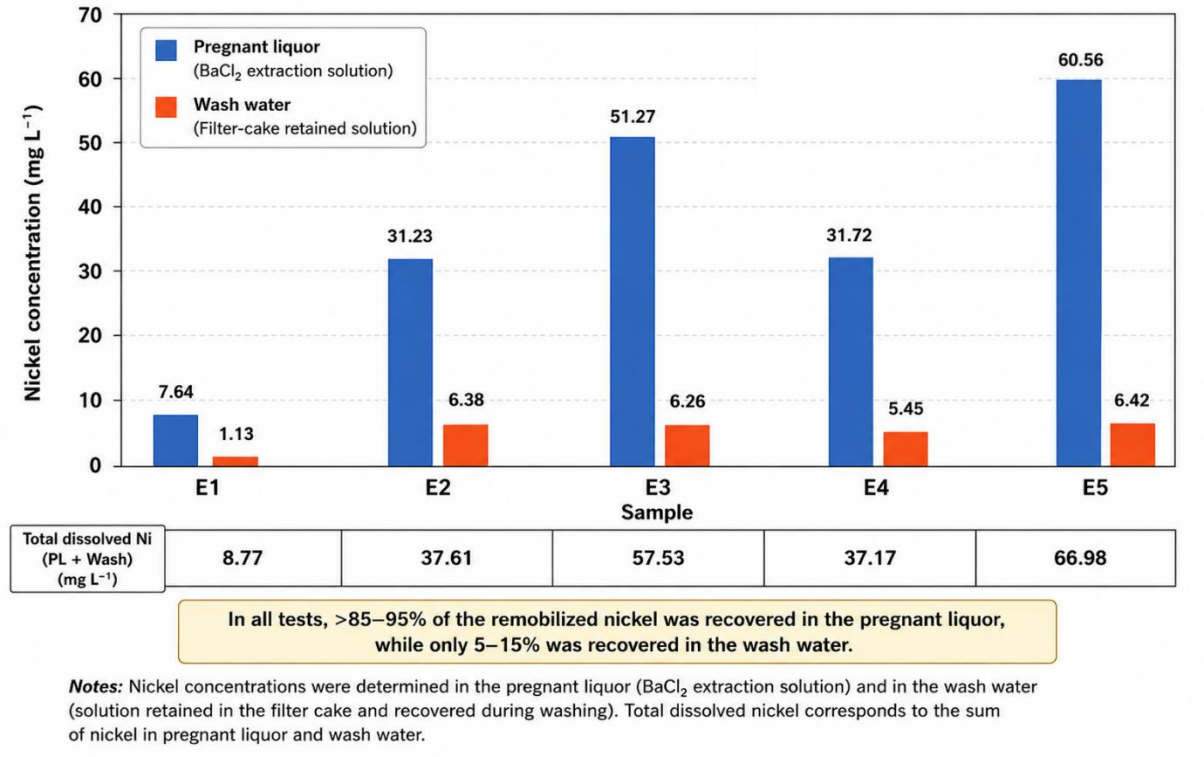


Figure 5. Comparison between nickel concentrations measured in pregnant liquors and wash water. Source: Prepared by the authors from ICP-OES analyses of pregnant liquors and wash-water samples collected during the $BaCl_2$ diagnostic treatment of atmospheric sulfuric leaching residues.

Figure 5 shows that nickel concentrations in the pregnant liquors were substantially higher than those measured in the corresponding wash waters for all investigated residues.

JIRRS
Journal International Review of Research Studies
Received: 02/05/2026 - **Accepted:** 25/06/2026
Vol: 01.09
DOI: 10.66104/x7rh8151
Pages: 1-39

Pregnant liquor concentrations ranged from 7.64 to 60.56 µg mL^{-1}, whereas wash-water concentrations varied from approximately 1.1 to 3.3 µg mL^{-1}. This difference indicates that most nickel release occurred during the $BaCl_2$ diagnostic treatment stage rather than during the subsequent washing step.

The presence of nickel in the wash-water streams indicates that part of the dissolved nickel remained entrained in the pore solution retained by the filter cake after solid–liquid separation. Therefore, including the wash-water contribution in the nickel balance is important to avoid underestimating the operationally defined $BaCl_2$-remobilizable nickel fraction.

Residues with higher nickel concentrations in the pregnant liquors generally also showed higher nickel concentrations in the wash waters. This relationship suggests that both streams were associated with the same dissolved nickel pool generated during the diagnostic treatment. However, because control tests were not available, the measured nickel cannot be attributed exclusively to sulfate-bearing host phases.

3.3. Quantification of $BaCl_2$-Remobilizable Nickel

The nickel inventory initially contained in each residue was calculated from the residue mass and nickel grade determined by chemical analysis. Nickel recovered in the pregnant liquors and wash waters was subsequently used to estimate the fraction of nickel remobilized during $BaCl_2$ treatment. The resulting solution-phase nickel balance is presented in Table 10.

Table 10. Nickel solution-phase balance and quantification of $BaCl_2$-remobilizable nickel during $BaCl_2$ treatment.

Test	Residue Ni Grade (%)	Initial Ni Inventory (mg)	Ni in Pregnant Liquor (mg)	Ni in Wash Water (mg)	$BaCl_2$-Remobilized Ni (mg)	Remobilized Ni (% of Initial Ni Inventory)
E1	0.641	961.5	6.1	1.1	7.2	0.75
E2	0.724	1086.0	28.2	6.4	34.6	3.18
E3	0.728	1092.0	45.3	6.3	51.6	4.73
E4	0.688	1032.0	27.9	5.4	33.3	3.23
E5	0.616	924.0	53.5	6.4	59.9	6.48
Average	—	—	—	—	37.3	3.67

Source: Calculated from residue chemical analyses, measured liquor volumes, wash-water volumes, and ICP-OES nickel determinations.
Note: Direct post-treatment solid nickel analyses were not available. Therefore, the remaining solid nickel inventory was inferred by difference, and mass-balance closure was not independently verified by direct analysis of all streams. Future work should include final residue nickel assays and report closure within an acceptable analytical uncertainty interval, preferably ±5-10%.

The values reported in Table 10 do not represent nickel extraction from the original ore. Instead, they represent the fraction of the initial residue nickel inventory released to solution

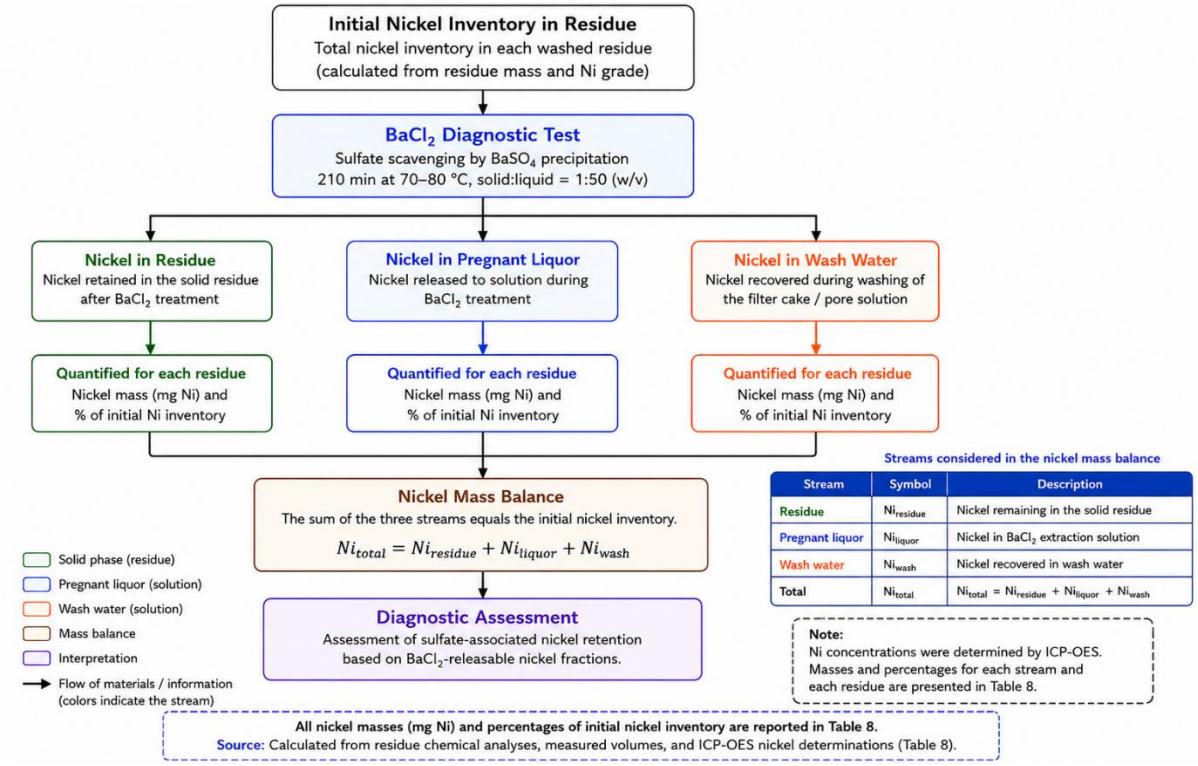
JIRRS
Journal International Review of Research Studies
Received: 02/05/2026 - **Accepted:** 25/06/2026
Vol: 01.09
DOI: 10.66104/x7rh8151
Pages: 1-39

under the experimental conditions employed following $BaCl_2$ addition. The combined nickel recovered in the pregnant liquor and wash-water streams was used as an operational indicator of nickel remobilization during treatment.

The amount of remobilized nickel varied substantially among the residues, ranging from 7.2 mg for E1 to 59.9 mg for E5. When expressed relative to the initial nickel inventory of each residue, the remobilized fraction ranged from 0.75 to 6.48%, with an average value of 3.67%. These results indicate that only a limited portion of the residual nickel inventory was mobilized during $BaCl_2$ treatment, whereas most nickel remained associated with the solid residue.

The variability among residues indicates differences in nickel phases' abundance and stability, affecting remobilization during sulfate scavenging. E5 showed the highest remobilized nickel, while E1 had the lowest, aligning with dissolved nickel levels and suggesting varied nickel retention mechanisms among residues.

To evaluate nickel distribution during the diagnostic treatment, an operational mass-balance framework was established. Nickel in the pregnant liquor and wash-water was directly quantified; remaining nickel in the solid was inferred by difference since direct analyses were unavailable. The mass-balance framework is shown in Figure 6.



JIRRS
Journal International Review of Research Studies
Received: 02/05/2026 - **Accepted:** 25/06/2026
Vol: 01.09
DOI: 10.66104/x7rh8151
Pages: 1-39

Figure 6. Nickel mass distribution among residue, pregnant liquor and wash-water streams. Source: Prepared by the authors based on nickel mass balance calculations performed for the $BaCl_2$ diagnostic extraction tests.

Figure 6 summarizes the methodology used to track nickel distribution during $BaCl_2$ treatment. The three terms considered comprise: (i) nickel remaining in the solid residue after treatment, estimated by difference, (ii) nickel released to the pregnant liquor during $BaCl_2$ extraction, and (iii) nickel recovered from the wash-water stream associated with solution retained in the filter cake. Because the final solid nickel grade was not measured directly, the balance should be regarded as an operational accounting framework rather than a fully closed analytical mass balance.

Separating nickel in the pregnant liquor from that in washing is crucial because some dissolved nickel may stay entrained in the pore solution within the filter cake after filtration. Including wash-water contribution improves the nickel release balance and prevents underestimating the remobilized fraction.

The proposed operational balance approach compares nickel remobilization in atmospheric leaching residues and evaluates $BaCl_2$-remobilizable nickel related to sulfate retention. While it doesn't identify specific mineral hosts for nickel, it offers a useful diagnostic tool for investigating nickel losses and optimizing hydrometallurgical processes.

3.4. Variability Among Atmospheric Leaching Residues

Substantial variability was observed among the atmospheric leaching residues despite their relatively similar bulk nickel grades. After $BaCl_2$ treatment, the dissolved nickel concentration measured at 210 min ranged from 7.64 to 60.56 µg mL^{-1}, corresponding to an approximately eight-fold variation among the residues. This behavior indicates that the operationally defined $BaCl_2$-remobilizable nickel fraction was not controlled solely by the total nickel content of the residues.

The observed variability is more likely related to differences in residue-specific properties, including mineralogical assemblage, sulfate association, crystallinity, surface chemistry, pore-solution retention, and the formation of secondary phases during sulfuric acid leaching. However, because replicate extraction tests and direct mineralogical confirmation were not available, these differences should be interpreted as exploratory evidence of variable remobilization behavior rather than as proof of a single nickel-retention mechanism.

JIRRS
Journal International Review of Research Studies
Received: 02/05/2026 - **Accepted:** 25/06/2026
Vol: 01.09
DOI: 10.66104/x7rh8151
Pages: 1-39

Therefore, the $BaCl_2$ extraction results provide an operational comparison of nickel remobilizability among residues. The marked differences in nickel release are consistent with local variations in solution chemistry, sulfate concentration, iron hydrolysis, and secondary phase formation, but they do not independently identify the nickel-bearing host phases. The quantitative variability observed among the residues is summarized in Table 11.

Table 11. Variability of $BaCl_2$-remobilizable nickel released from atmospheric leaching residues during $BaCl_2$ treatment

Residue	Dissolved Ni after 210 min (µg mL^{-1})	Relative to E1 (×)	$BaCl_2$-remobilizable Ni classification
E1	7.64	1.00	Very Low
E2	31.23	4.09	Moderate
E3	51.27	6.71	High
E4	31.72	4.15	Moderate
E5	60.56	7.93	Very High

Parameter	Value
Number of residues (n)	5
Minimum (µg mL^{-1})	7.64
Maximum (µg mL^{-1})	60.56
Mean (µg mL^{-1})	36.48
Standard deviation (µg mL^{-1})	21.32
Coefficient of variation (%)	58.4
Maximum/Minimum ratio	7.93
Variability range (µg mL^{-1})	52.92

Table 11 shows significant heterogeneity in dissolved nickel release among residues. The 58.4% variation reflects between-sample differences, not experimental reproducibility, since $BaCl_2$ replicates were not done. Residues E3 and E5 released the most nickel, while E1 released the least. This supports using $BaCl_2$ as a diagnostic tool for comparing residues, but highlights the need for replicate testing and further solid-phase analysis in future research.

Figure 7 summarizes the final dissolved nickel concentrations obtained after $BaCl_2$ treatment for the five atmospheric leaching residues investigated.

JIRRS
Journal International Review of Research Studies
Received: 02/05/2026 - **Accepted:** 25/06/2026
Vol: 01.09
DOI: 10.66104/x7rh8151
Pages: 1-39

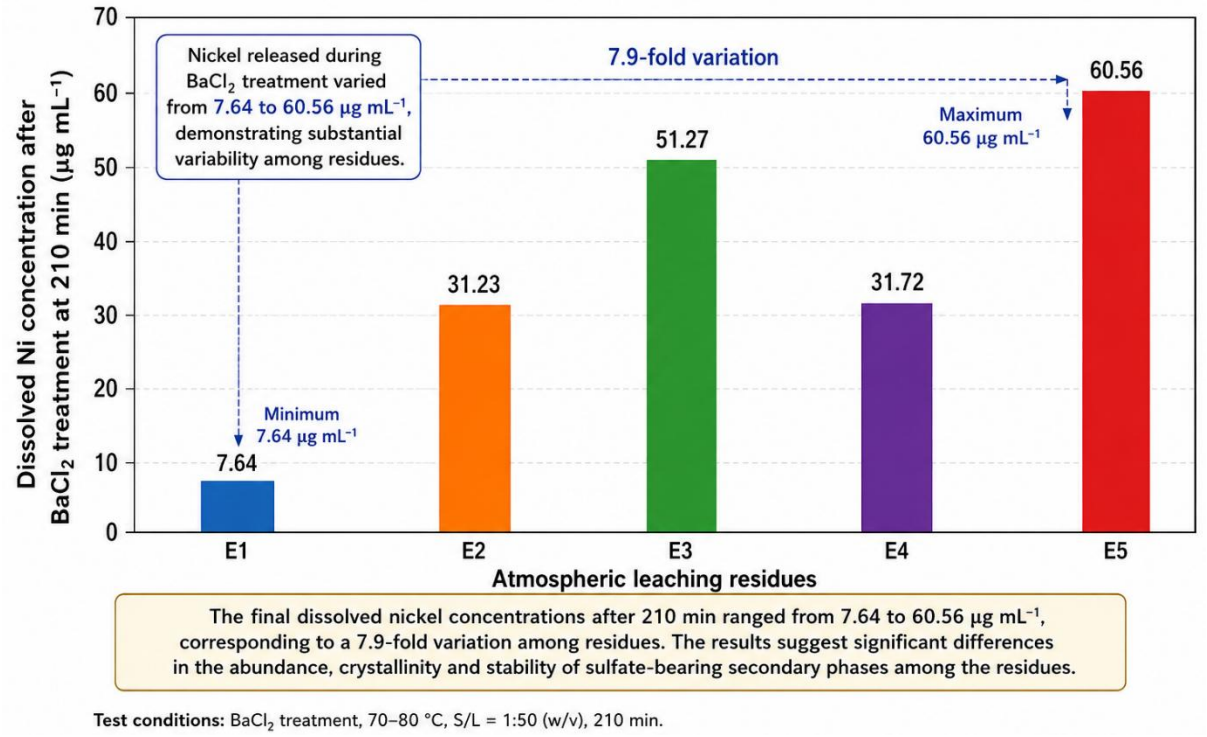


Figure 7. Variability of nickel released during $BaCl_2$ treatment of atmospheric leaching residues. Source: ICP-OES analyses of intermediate liquors collected during $BaCl_2$ treatment of atmospheric leaching residues (this study)

The highest dissolved nickel concentration was observed for residue E5 (60.56 µg mL^{-1}), followed by E3 (51.27 µg mL^{-1}), whereas E1 exhibited the lowest value (7.64 µg mL^{-1}). Intermediate concentrations were measured for E2 (31.23 µg mL^{-1}) and E4 (31.72 µg mL^{-1}). The similarity between E2 and E4 suggests comparable $BaCl_2$-remobilizable responses in these two residues.

The variation among residues shows that the $BaCl_2$-remobilizable nickel fraction was unevenly distributed, supporting the idea that some nickel was retained in labile secondary environments influenced by local precipitation and washing conditions. Therefore, dissolved nickel after $BaCl_2$ treatment can serve as a practical indicator of relative remobilizability, not as an exact measure of $BaCl_2$-remobilizable nickel.

These findings suggest that sulfate-bearing or iron-associated secondary phases may contribute to nickel retention in atmospheric leaching residues. Therefore, controlling iron hydrolysis, sulfate chemistry, filtration, and washing conditions may provide opportunities to reduce nickel losses, although these process implications require validation using controls, sulfate balances, and mineralogical evidence.

JIRRS
Journal International Review of Research Studies
Received: 02/05/2026 - **Accepted:** 25/06/2026
Vol: 01.09
DOI: 10.66104/x7rh8151
Pages: 1-39

3.5. Exploratory Relationship Between Residual Iron and $BaCl_2$-Remobilizable Nickel

Residual iron contents and dissolved nickel concentrations are presented in Table 12.

Table 102. Relationship between residual iron content and dissolved nickel concentration after 210 min of $BaCl_2$ treatment

Test	Residual Fe (wt.%)	Dissolved Ni at 210 min (μg mL^{-1})
E1	37.4	7.64
E2	39.0	31.23
E3	38.1	51.27
E4	37.0	31.72
E5	33.8	60.56

Source: Residual iron contents determined by chemical analysis of atmospheric sulfuric leaching residues and dissolved nickel concentrations measured in extraction liquors after 210 min of $BaCl_2$ treatment.

The data presented in Table 12 show considerable variability in dissolved nickel concentration despite relatively similar iron contents among the investigated residues. Residual iron contents ranged from 33.8 to 39.0 wt.%, whereas dissolved nickel concentrations varied from only 7.64 to 60.56 μg mL^{-1}.

The lack of a simple relationship between iron and dissolved nickel shows total iron alone cannot explain nickel remobilization during $BaCl_2$ treatment. Instead, nickel retention depends on mineralogical traits of iron-bearing residues, like crystallinity, sulfate, surface area, and nickel incorporation.

High dissolved nickel in Tests 3 and 5, together with limited remobilization in Test 1, suggests that total residual iron is not a sufficient descriptor of nickel remobilization. The data are more consistent with a role of iron speciation, crystallinity, sulfate association, surface area, and local precipitation history than with total Fe content alone.

The results support $BaCl_2$'s usefulness in identifying residues with larger labile nickel fractions, though bulk chemistry alone cannot pinpoint responsible solid phases. An inverse relationship was observed between residual iron and remobilized nickel.

Because the dataset contains only five residues, the relationship was treated as exploratory. Pearson correlation between residual Fe and dissolved Ni at 210 min was $r = -0.51$ ($p = 0.38$), and Spearman correlation was $\rho = -0.50$ ($p = 0.39$). These values do not support robust statistical inference, but they indicate that total Fe is a poor proxy for the reactive iron phases controlling nickel retention.

This interpretation is consistent with mechanisms reported in previous studies, but the following possible hosts were not directly confirmed in the present work:

JIRRS
Journal International Review of Research Studies
Received: 02/05/2026 - **Accepted:** 25/06/2026
Vol: 01.09
DOI: 10.66104/x7rh8151
Pages: 1-39

- ferric sulfates;
- basic ferric sulfates;
- jarosite-type compounds;
- ferrihydrite;
- poorly crystalline goethite.

To examine the link between residue composition and remobilizable nickel, dissolved nickel after 210 min of $BaCl_2$ treatment was compared with residual iron in each sulfuric leaching residue. Iron was considered because ferric sulfates, basic ferric sulfates, and iron oxyhydroxides may act as nickel sinks in acidic sulfate systems. The exploratory correlation is shown in Figure 8.

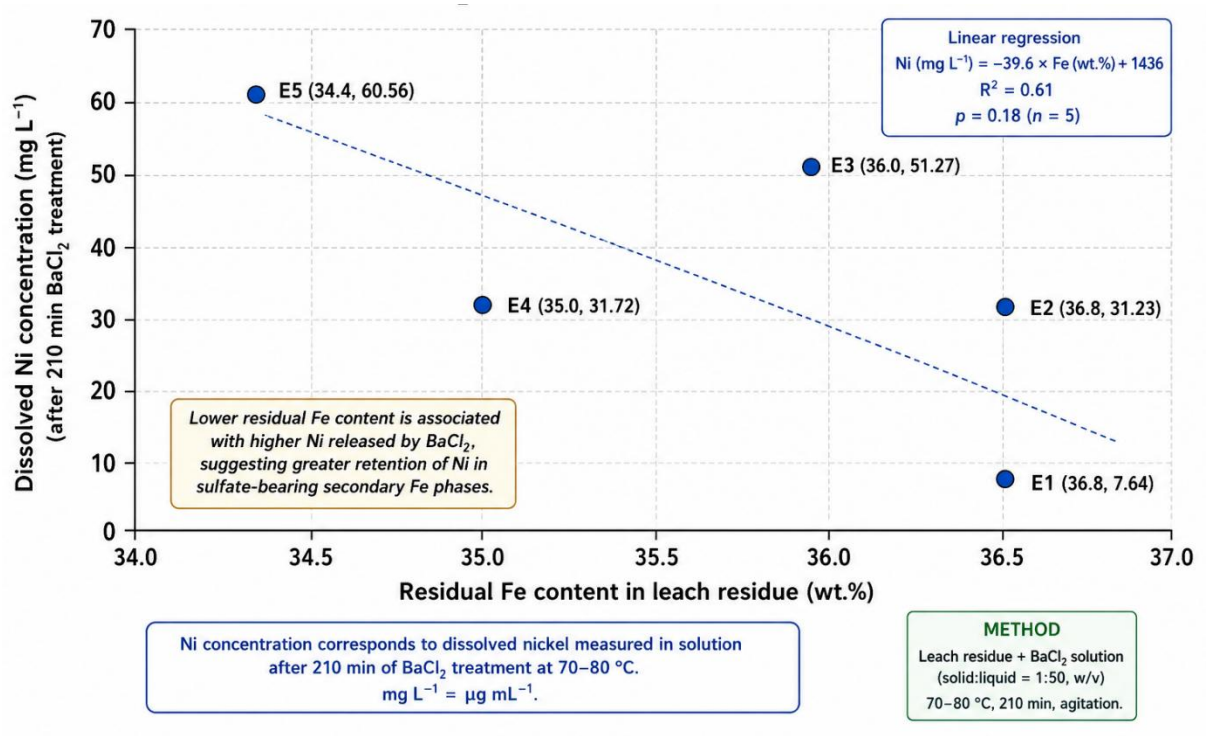


Figure 8. Relationship between residual iron content and dissolved nickel concentration. Source: Prepared by the authors from experimental $BaCl_2$ extraction tests performed on atmospheric sulfuric leaching residues generated from ferruginous nickel ore processing.

Figure 8 suggests a weak tendency for higher dissolved nickel concentrations to be associated with lower residual iron contents. However, because n = 5 and the correlation is not statistically significant, the trend should be interpreted cautiously and used only as an exploratory indication.

JIRRS
Journal International Review of Research Studies
Received: 02/05/2026 - **Accepted:** 25/06/2026
Vol: 01.09
DOI: 10.66104/x7rh8151
Pages: 1-39

The relationship is consistent with the broader understanding that dissolved nickel may be retained by ferric hydroxy-sulfates, jarosite-like compounds, poorly crystalline iron oxyhydroxides, mixed Fe-Ni sulfate environments, adsorption, or occlusion. The present dataset does not distinguish among these mechanisms.

The results further indicate that total iron content alone is not sufficient to explain nickel retention. Mineralogical characteristics such as crystallinity, sulfate content, specific surface area, and the degree of nickel incorporation or adsorption likely influence the amount of remobilizable nickel in each residue. Consequently, $BaCl_2$ treatment provides comparative diagnostic information regarding sulfate-related nickel remobilization, but it does not replace direct solid-phase speciation.

3.6. Operational Evidence for $BaCl_2$-Remobilizable Nickel During Atmospheric Sulfuric Acid Leaching

The feed ore contained approximately 1.00 wt.% Ni, whereas the leaching residues contained between 0.616 and 0.728 wt.% Ni.

These results indicate that sulfuric acid leaching extracted a substantial fraction of the original nickel inventory.

However, subsequent $BaCl_2$ treatment released an additional fraction corresponding to 0.75-6.48% of the initial nickel inventory present in the residues, with an average of 3.67%.

Because $BaCl_2$ is not a conventional nickel-leaching reagent under the conditions employed, the observed nickel release is consistent with the presence of a chemically labile nickel fraction affected by sulfate scavenging. Nevertheless, the release cannot be treated as direct mineralogical proof of co-precipitation without control tests, sulfate balance, and post-treatment solid characterization.

Potential, but unconfirmed, nickel-retention environments include:

- $NiSO_4 \cdot xH_2O$;
- Fe–Ni sulfate phases;
- basic ferric sulfates;
- sulfate-bearing goethite;
- sulfate-bearing ferrihydrite;
- adsorbed nickel on iron oxyhydroxide surfaces.

JIRRS
Journal International Review of Research Studies
Received: 02/05/2026 - **Accepted:** 25/06/2026
Vol: 01.09
DOI: 10.66104/x7rh8151
Pages: 1-39

These observations are consistent with sulfate-related retention mechanisms discussed by Pereira (2026b), but the present data should be interpreted as operational evidence rather than definitive host-phase identification.

3.7. Thermodynamic Basis of $BaCl_2$-Induced Nickel Remobilization

The first step of the process is dissolution of barium chloride:

$$BaCl_2 \rightarrow Ba^{2+} + 2Cl^- \quad \text{Equation 6}$$

Thermodynamic calculations indicate that this reaction is favorable over the experimental temperature range under the simplified standard-state assumptions used in this study.

At 70–80 °C:

$$\Delta G = -2.87 \text{ to } -2.74 \text{ kcal/mol}$$

$$\log K = 1.83 \text{ to } 1.70$$

supporting the availability of dissolved barium ions under the simplified assumptions used.

The first step of the proposed nickel remobilization mechanism involves dissolution and dissociation of barium chloride in the aqueous medium. The release of Ba^{2+} ions is essential because these ions subsequently react with sulfate species to form highly insoluble barium sulfate. Therefore, evaluation of the thermodynamic behavior of $BaCl_2$ dissociation provides important information regarding the availability of dissolved barium under the experimental conditions. Thermodynamic parameters calculated for the dissociation reaction between 70 and 80 °C are presented in Table 13

Table 13. Thermodynamic parameters for $BaCl_2$ dissociation

Temperature (°C)	ΔH (kcal mol^{-1})	ΔS (cal mol^{-1} K^{-1})	ΔG (kcal mol^{-1})	Equilibrium Constant, K	log K
70	-6.993	-12.013	-2.871	6.743×10^1	1.829
75	-7.403	-13.196	-2.808	5.794×10^1	1.763
80	-7.816	-14.376	-2.739	4.959×10^1	1.695

Source: Thermodynamic calculations performed for $BaCl_2$ dissociation in aqueous solution within the experimental temperature range employed in this study.

The thermodynamic results demonstrate that $BaCl_2$ dissociation is spontaneous throughout the investigated temperature range. Gibbs free energy values remain negative, ranging from −2.87 to −2.74 kcal mol^{-1} between 70 and 80 °C, indicating favorable formation of dissolved Ba^{2+} and Cl^- ions.

The equilibrium constants vary from approximately 50 to 67, with log K values between 1.70 and 1.83. Although the equilibrium constant decreases slightly with increasing

JIRRS
Journal International Review of Research Studies
Received: 02/05/2026 - **Accepted:** 25/06/2026
Vol: 01.09
DOI: 10.66104/x7rh8151
Pages: 1-39

temperature, the dissociation reaction remains strongly favored under all experimental conditions employed in this study.

These results indicate that $BaCl_2$ acts as an effective source of dissolved barium ions during the extraction tests. Consequently, the availability of Ba^{2+} is not expected to limit sulfate removal or nickel remobilization. Instead, the overall process is controlled primarily by the subsequent precipitation of $BaSO_4$, which constitutes the principal thermodynamic driving force for sulfate scavenging and release of nickel associated with secondary sulfate-bearing phases.

The combination of favorable $BaCl_2$ dissociation (Table 13), favorable $BaSO_4$ precipitation (Table 14), and favorable conversion of $NiSO_4 \cdot 6H_2O$ into dissolved Ni^{2+} (Table 15) provides a chemically plausible thermodynamic framework for nickel release during $BaCl_2$ treatment. However, these calculations should be regarded as standard-state screening calculations. They do not constitute a full aqueous speciation model including activities, ionic strength, chloride complexation, HSO_4^-/SO_4^{2-} distribution, $NiSO_4(aq)$, $NiHSO_4^+$, $BaCl^+$, or temperature-dependent non-ideal behavior.

3.8. Sulfate Scavenging by $BaSO_4$ Precipitation

The key thermodynamic driving force of the process is precipitation of barium sulfate:

$$Ba^{2+}\,(aq) + SO_4^{2-}\,(aq) \rightarrow BaSO_4\,(s) \qquad \text{Equation 7}$$

At 70–80 °C:

$$\Delta G = -13.7 \text{ to } -14.1 \text{ kcal/mol}$$

$$K \approx 5 \times 10^8$$

indicating an extremely favorable reaction.

The very large equilibrium constant indicates that sulfate removal by $BaSO_4$ precipitation is strongly favored under the simplified thermodynamic representation.

The driving force proposed for nickel remobilization during $BaCl_2$ treatment is the precipitation of barium sulfate. Because $BaSO_4$ has very low solubility, its formation may remove sulfate species from solution and shift equilibria involving labile sulfate-associated nickel toward dissolution. This interpretation is consistent with the observed nickel release but requires sulfate measurements and activity-based speciation modeling to rigorously validate it (Table 14).

Table 114. Thermodynamic parameters for $BaSO_4$ precipitation

JIRRS
Journal International Review of Research Studies
Received: 02/05/2026 - **Accepted:** 25/06/2026
Vol: 01.09
DOI: 10.66104/x7rh8151
Pages: 1-39

Temperature (°C)	ΔH (kcal mol^{-1})	ΔS (cal mol^{-1} K^{-1})	ΔG (kcal mol^{-1})	Equilibrium constant, K	log K
70	-0.773	37.711	-13.714	5.432×10^8	8.735
75	-0.337	38.974	-13.906	5.368×10^8	8.730
80	0.104	40.230	-14.104	5.356×10^8	8.729

Source: Thermodynamic calculations performed for the Ba^{2+}–SO_4^{2-}–$BaSO_4$ system in the experimental temperature range.

The results presented in Table 14 demonstrate that $BaSO_4$ precipitation is strongly thermodynamically favored throughout the investigated temperature range in the simplified reaction model. Gibbs free energy values remain highly negative, varying from -13.71 to -14.10 kcal mol^{-1} between 70 and 80 °C.

The exceptionally high equilibrium constants, on the order of 10^8, further confirm the strong tendency of Ba^{2+} ions to react with sulfate ions and form barite. Although a slight decrease in log K is observed with increasing temperature, the magnitude of the equilibrium constant remains sufficiently large to ensure nearly complete sulfate removal from solution.

These thermodynamic results are useful for interpreting the experimental response because sulfate consumption via $BaSO_4$ formation can render labile, sulfate-associated nickel environments less stable. However, the thermodynamic calculations cannot prove that the nickel detected in the extraction liquors originated from a specific secondary sulfate phase rather than from other labile sources.

3.9. Destabilization of Nickel Sulfate Phases

The thermodynamic response of nickel sulfate to sulfate scavenging can be represented by:

$$Ba^{2+} + NiSO_4 \cdot 6H_2O \rightarrow BaSO_4(s) + Ni^{2+} + 6H_2O \qquad \text{Equation 8}$$

At 70–80 °C:

$$\Delta G = -10.59 \text{ to } -10.86 \text{ kcal/mol}$$

$$K = 5.3 \times 10^6$$

$$\log K \approx 6.7$$

These values indicate that the conversion of nickel sulfate to dissolved nickel ions, coupled with $BaSO_4$ precipitation, is thermodynamically favored in the simplified model. Therefore, the observed nickel release is consistent with destabilization of sulfate-bearing nickel environments, but direct leaching, chloride effects, and desorption cannot be excluded without controls.

To further investigate the mechanism potentially responsible for nickel remobilization during $BaCl_2$ treatment, the thermodynamics of the reaction between dissolved barium ions

JIRRS
Journal International Review of Research Studies
Received: 02/05/2026 - **Accepted:** 25/06/2026
Vol: 01.09
DOI: 10.66104/x7rh8151
Pages: 1-39

and hydrated nickel sulfate were evaluated. This reaction represents a simplified model for the destabilization of a labile sulfate-associated nickel species via transfer of sulfate to the highly stable $BaSO_4$ phase. The calculated thermodynamic parameters within the experimental temperature range (70-80 °C) are presented in Table 15.

Table 125. Thermodynamic parameters for conversion of $NiSO_4 \cdot 6H_2O$ into $BaSO_4$ and dissolved Ni^{2+}. Source: Thermodynamic calculations performed for the Ba^{2+}–$NiSO_4$–SO_4^{2-} system under conditions representative of the experimental temperature range employed in this study

Temperature (°C)	ΔH (kcal mol^{-1})	ΔS (cal mol^{-1} K^{-1})	ΔG (kcal mol^{-1})	Equilibrium Constant (K)	log K
70	-1.748	25.778	-10.594	5.595×10^6	6.748
75	-1.504	26.485	-10.725	5.407×10^6	6.733
80	-1.263	27.172	-10.859	5.256×10^6	6.721

The results demonstrate that the conversion of hydrated nickel sulfate into dissolved nickel ions and barium sulfate is strongly spontaneous throughout the experimental temperature range. Gibbs free energy values remained highly negative (−10.59 to −10.86 kcal mol^{-1}), while equilibrium constants remained on the order of 10^6, indicating a strong thermodynamic preference for sulfate transfer from nickel sulfate to barium sulfate.

These results provide thermodynamic support for the proposed mechanism. Once Ba^{2+} is introduced into the system, sulfate associated with labile nickel-bearing species may be preferentially incorporated into $BaSO_4$, shifting equilibria toward dissolved Ni^{2+}. This standard-state interpretation should be validated in future work using an aqueous speciation model such as PHREEQC, HSC Chemistry, Medusa/Hydra, or an equivalent activity-based approach.

The large equilibrium constants observed between 70 and 80 °C support the concept that $BaCl_2$ acts primarily as a sulfate scavenger rather than as a conventional nickel-leaching reagent. Therefore, the $BaCl_2$ treatment can reveal a labile remobilizable fraction, while stronger claims about co-precipitation require independent controls and solid-phase confirmation.

The experimental results indicate that nickel release during $BaCl_2$ treatment is consistent with a sequence of sulfate-scavenging reactions. Dissolution of $BaCl_2$ provides Ba^{2+} ions, which may react with sulfate species to form highly insoluble barium sulfate. Removal of sulfate can decrease sulfate activity and shift equilibria involving labile sulfate-associated nickel toward dissolved Ni^{2+}. Consequently, $BaCl_2$ is treated here as a diagnostic sulfate-scavenging reagent. The conceptual thermodynamic mechanism proposed for nickel remobilization is illustrated in Figure 9.

JIRRS
Journal International Review of Research Studies
Received: 02/05/2026 - **Accepted:** 25/06/2026
Vol: 01.09
DOI: 10.66104/x7rh8151
Pages: 1-39

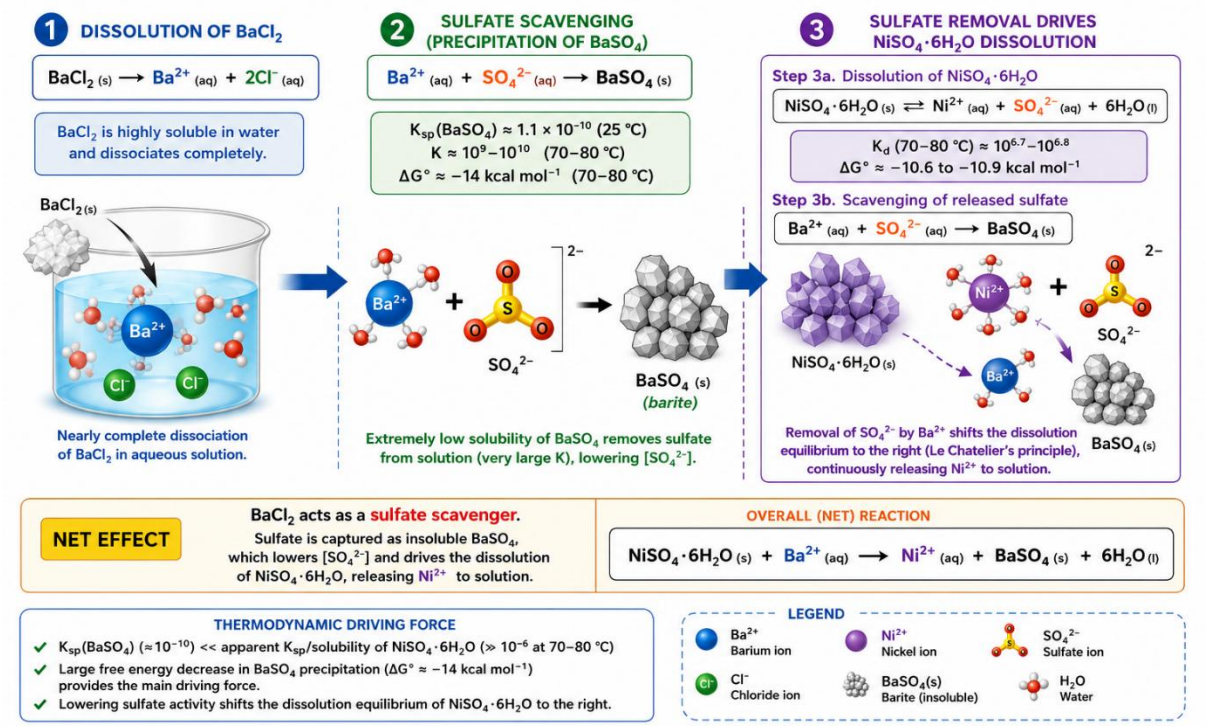


Figure 9. Thermodynamic mechanism of sulfate scavenging and nickel remobilization induced by $BaCl_2$.

3.10. Implications for Diagnostic Quantification of $BaCl_2$-Remobilizable Nickel

The results suggest that conventional nickel recovery calculations based exclusively on dissolved nickel concentrations may underestimate nickel that was temporarily dissolved and then retained in labile secondary environments. The magnitude of this effect must be confirmed by control experiments, sulfate balances, and solid-phase characterization.

A portion of dissolved nickel can be temporarily immobilized through:

- sulfate precipitation;
- adsorption on iron oxyhydroxides;
- incorporation into Fe–Ni sulfate phases;
- co-precipitation with ferric hydrolysis products.

The $BaCl_2$ methodology developed in this work provides a practical diagnostic tool for estimating this hidden, operationally defined nickel inventory.

The experimental evidence obtained in this study indicates that a measurable fraction of residual nickel can be remobilized during $BaCl_2$ treatment. The method was developed as a diagnostic tool to evaluate nickel release under sulfate-scavenging conditions. Figure 10

JIRRS
Journal International Review of Research Studies
Received: 02/05/2026 - **Accepted:** 25/06/2026
Vol: 01.09
DOI: 10.66104/x7rh8151
Pages: 1-39

summarizes the conceptual model describing nickel dissolution, possible secondary retention, sulfate removal by barium ions, and subsequent nickel remobilization.

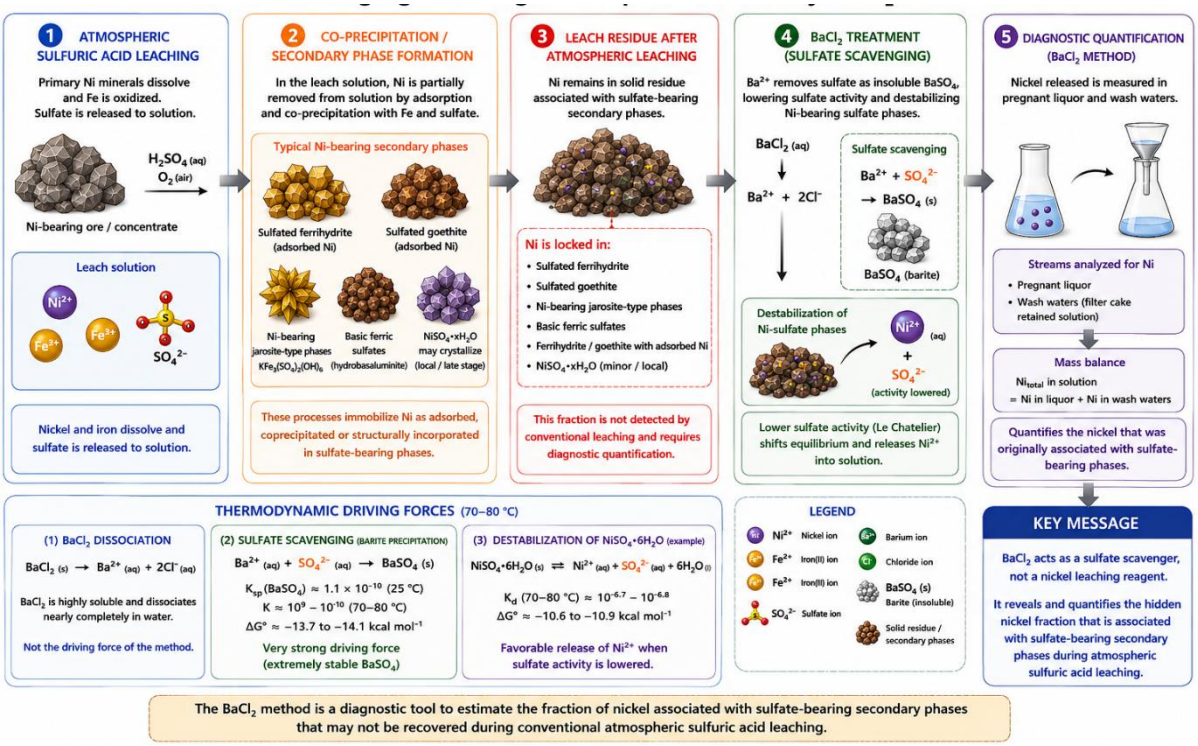


Figure 10. Conceptual model showing nickel dissolution, possible secondary retention, sulfate scavenging and diagnostic quantification by $BaCl_2$ treatment.

The conceptual model presented in Figure 10 integrates the experimental observations and thermodynamic screening calculations developed in this investigation. The model highlights that $BaCl_2$ does not function here as an industrial nickel-recovery reagent but rather as a diagnostic sulfate scavenger, revealing a labile nickel fraction retained in the residue under the tested conditions.

The results support the interpretation that a measurable fraction of the residual nickel inventory was associated with labile environments susceptible to $BaCl_2$-induced remobilization. By removing sulfate from solution through barite precipitation, the $BaCl_2$ treatment provides a practical experimental approach for estimating this operational fraction. The methodology may therefore be used as a diagnostic tool to compare residues and support optimization studies, but it should be coupled with controls, sulfate measurements, and mineralogical characterization before strong mechanistic conclusions are drawn.

The $BaCl_2$ extraction methodology quantifies only the nickel fraction remobilized under the experimental conditions employed. More stable nickel-bearing phases may remain

JIRRS
Journal International Review of Research Studies
Received: 02/05/2026 - **Accepted:** 25/06/2026
Vol: 01.09
DOI: 10.66104/x7rh8151
Pages: 1-39

unaffected, and therefore the reported values should be interpreted as operational estimates of a labile fraction rather than as total sulfate-associated nickel retention.

The principal boundary of this work is the distinction between operational extraction and mineralogical proof. The $BaCl_2$ test quantifies nickel released under defined acidic, heated, sulfate-scavenging conditions. It does not independently identify whether the released nickel was hosted by hydrated nickel sulfate, mixed Fe-Ni sulfates, jarosite-like phases, ferrihydrite, goethite, adsorbed surface complexes, or entrained pore solution.

The absence of replicate $BaCl_2$ tests, acidified-water controls, chloride-only controls, residue-without-$BaCl_2$ controls, sulfate before/after measurements, residual Ba^{2+} measurements, and post-treatment solid analyses limits mechanistic attribution. Consequently, variability among residues is interpreted as exploratory evidence of distinct remobilization behavior rather than definitive proof of distinct co-precipitation intensities.

The thermodynamic calculations support the feasibility of sulfate scavenging by $BaSO_4$ precipitation, but they are simplified standard-state calculations. Future work should include activity-based aqueous speciation, sulfate and barium balances, XRD/SEM-EDS/FTIR or sequential extraction, and replicate tests for high-, medium-, and low-response residues.

4. Industrial Implications

The results indicate that nickel losses during atmospheric sulfuric acid leaching should not be attributed exclusively to incomplete dissolution of primary or refractory nickel-bearing minerals. A measurable fraction of the residual nickel inventory was remobilized under $BaCl_2$ sulfate-scavenging conditions, suggesting that secondary retention mechanisms may also contribute to nickel remaining in leach residues. This interpretation is relevant for process diagnosis because nickel losses may occur not only during the dissolution stage, but also during subsequent cooling, filtration, washing, neutralization, precipitation, or impurity-removal steps (Amorim et al., 2022; Pereira, 2026a).

From an industrial perspective, this finding has several implications. First, part of the nickel loss in atmospheric leaching circuits may occur after nickel has already entered solution, followed by retention in secondary sulfate-bearing or iron-rich environments. Second, optimization of iron precipitation, impurity removal, and residue washing stages may improve overall nickel recovery by reducing secondary nickel retention. Third, diagnostic $BaCl_2$ extraction may provide a practical method for estimating an operationally defined remobilizable nickel fraction in atmospheric leaching residues. Finally, historical residues may

JIRRS
Journal International Review of Research Studies
Received: 02/05/2026 - **Accepted:** 25/06/2026
Vol: 01.09
DOI: 10.66104/x7rh8151
Pages: 1-39

contain nickel associated with labile secondary environments, although their recovery potential must be evaluated separately through techno-economic, environmental, and regulatory assessments.

The average remobilizable nickel fraction measured in this study corresponded to 3.67% of the initial residue nickel inventory. Although this value is limited in absolute terms, it indicates that process optimization aimed at reducing secondary nickel retention could be meaningful in selected cases, particularly where large residue inventories are generated or where nickel prices justify additional diagnostic evaluation. Nevertheless, $BaCl_2$ treatment should not be interpreted as an industrial nickel-recovery route at this stage. Its practical application would require detailed assessment of reagent cost, barium toxicity, barite waste handling, sulfate balance, water management, and integration with existing hydrometallurgical circuits.

These implications are consistent with studies showing that downstream purification, neutralization, solvent extraction, and precipitation stages can strongly influence the behavior of nickel, cobalt, manganese, iron, aluminum, and other impurities in lateritic hydrometallurgical circuits (Amorim et al., 2022; Dwi et al., 2025; Pereira, 2026a; Pereira, 2026b; Wen et al., 2024; Yun et al., 2025; Tayip et al., 2026; Wang et al., 2025). Therefore, the diagnostic identification of remobilizable nickel fractions can support broader efforts to improve metallurgical accounting and reduce avoidable nickel losses during downstream processing.

Although the present study does not evaluate product synthesis, the identification of a remobilizable nickel fraction may also support future studies on the recovery of nickel from intermediate streams and residues. In such cases, additional work would be required to determine whether remobilized nickel could be integrated into existing purification circuits or converted into marketable products such as nickel sulfate or nickel carbonate (Ananda et al., 2024; Wijenayake et al., 2025).

5. Conclusions

The present study showed that atmospheric sulfuric acid leaching residues contain a measurable fraction of nickel that can be remobilized under $BaCl_2$ sulfate-scavenging conditions. Although the original atmospheric leaching operation reduced the nickel grade of the ferruginous ore from approximately 1.00 wt.% to 0.616-0.728 wt.% in the final residues,

JIRRS
Journal International Review of Research Studies
Received: 02/05/2026 - **Accepted:** 25/06/2026
Vol: 01.09
DOI: 10.66104/x7rh8151
Pages: 1-39

subsequent treatment with barium chloride released a limited additional nickel fraction to solution.

Nickel concentrations released during $BaCl_2$ treatment ranged from 7.64 to 60.56 µg mL^{-1} at the final reported kinetic sampling time of 210 min, demonstrating the presence of a $BaCl_2$-remobilizable nickel fraction within all investigated residues. The rapid dissolution kinetics observed during the first stages of treatment, combined with the thermodynamic driving force associated with $BaSO_4$ precipitation, are consistent with sulfate-scavenging-induced nickel release.

The results further showed significant between-residue variability despite relatively similar nickel grades. This variability suggests that nickel remobilization depends on residue-specific properties such as secondary phase abundance, sulfate association, crystallinity, adsorption capacity, washing efficiency, and pore-solution retention, rather than on total nickel content alone. Because replicate tests were not performed, the variability should be interpreted as exploratory.

Thermodynamic evaluation indicated that $BaCl_2$ dissociation and $BaSO_4$ precipitation are favorable under the simplified standard-state assumptions employed. The coupled reaction involving conversion of $NiSO_4 \cdot 6H_2O$ into $BaSO_4$ and dissolved Ni^{2+} was also favorable. These calculations support the plausibility of the diagnostic mechanism but do not replace activity-based aqueous speciation or direct sulfate/barium balances.

The combined experimental and thermodynamic results provide operational evidence that a portion of the residual nickel inventory is susceptible to remobilization following sulfate scavenging. The $BaCl_2$-remobilizable fraction ranged from 0.75 to 6.48% of the initial nickel inventory in the residues, with an average of 3.67%. Therefore, $BaCl_2$ treatment can serve as a practical diagnostic tool to compare nickel remobilization behavior among leaching residues. However, definitive attribution to nickel co-precipitation requires additional controls, replicate testing, sulfate measurements, post-treatment solid analysis, and mineralogical characterization.

Declarations

Funding

The author declares that no specific funding was received for this study.

Conflicts of Interest

JIRRS
Journal International Review of Research Studies
Received: 02/05/2026 - **Accepted:** 25/06/2026
Vol: 01.09
DOI: 10.66104/x7rh8151
Pages: 1-39

The author declares that there are no known competing financial interests or personal relationships that could have appeared to influence the work reported in this paper.

Ethical Approval

This study did not involve human participants, human data, human biological material, or animals. Therefore, ethical approval was not required.

Author Contributions

Antonio Clareti Pereira was responsible for conceptualization, experimental data interpretation, methodology, calculations, data analysis, writing, review, and final approval of the manuscript.

References

1. Abdollahi, H., Hosseini-Nasab, M., & Yadollahi, A. (2024). *Bioleaching of lateritic nickel ores*. In *Biotechnological innovations in the mineral-metal industry* (pp. 41–66). Springer. https://doi.org/10.1007/978-3-031-43625-3_3.
2. Amorim, L. H. M., Aliprandini, P., Botelho Júnior, A. B., Jimenez Correa, M. M., & Espinosa, D. C. R. (2022). *Effect of impurities in the recovery of critical metals: The case of nickel laterite in the solvent extraction process*. *Journal of Sustainable Metallurgy, 8*(3), 1089–1102. https://doi.org/10.1007/s40831-022-00510-2.
3. Ananda, M. B., Vidathya, I. G. N. D., Ramadhani, M., Abdul, F., & Pintowantoro, S. (2024). *Effect of the pH with NaOH additives on the precipitation process of ferronickel leaching products from mini blast furnaces for $NiSO_4 \cdot 6H_2O$ synthesis*. *Sādhanā, 49*(1), Article 9. https://doi.org/10.1007/s12046-023-02377-9.
4. Caetano, G. C., Ostroski, I. C., & Barros, M. A. S. D. (2024). *Lateritic nickel and cobalt recovery routes: Strategic technologies*. *Mineral Processing and Extractive Metallurgy Review, 46*(3), 400–414. https://doi.org/10.1080/08827508.2024.2328696.
5. Caetano, G. C., Rodrigues, F. C., Ostroski, I. C., & Barros, M. A. S. D. (2025). *Low-cost alternative for iron recovery in lateritic nickel production by using ferronickel refining slag and kiln dust for iron precipitation from acid leachate*. *Hydrometallurgy, 237*, Article 106547. https://doi.org/10.1016/j.hydromet.2025.106547.
6. Chen, J., Zhong, Y., Luo, J., Zhang, X., Rao, M., Peng, Z., Li, G., & Jiang, T. (2026). *Enhanced selective leaching of Ni and Co via pre-oxidizing and high-pressure acid leaching of Ni-Co-Fe powder*. *Hydrometallurgy, 242*, Article 106709. https://doi.org/10.1016/j.hydromet.2026.106709.
7. Das, G., & Li, J. (2023). *Iron removal as goethite from synthetic laterite leach solutions*. *ACS Omega, 8*(13), 11805–11815. https://doi.org/10.1021/acsomega.2c07595.
8. Dwi, A., Zeng, W., & Xu, P. (2025). *Optimization and comparative analysis of neutralization agents for iron, aluminum, and chromium removal in HPAL pregnant leach solution*. *JOM, 77*(10). https://doi.org/10.1007/s11837-025-07699-z.

JIRRS
Journal International Review of Research Studies
Received: 02/05/2026 - **Accepted:** 25/06/2026
Vol: 01.09
DOI: 10.66104/x7rh8151
Pages: 1-39

9. Engelbrecht, E. (2025). Modelling the Hydrothermal Iron Removal Process at Rustenburg Base Metals Refinery to Enable Real-Time Acidity Control. In: Ni-Co 2025, 6th International Symposium on Nickel and Cobalt. NICO 2025. Springer, Cham. https://doi.org/10.1007/978-3-032-00167-2_3.
10. Ester, J., Pattanaik, A., Pradhan, N., & Sukla, L. B. (2020). *Applications of dissimilatory iron reducing bacteria (DIRB) for recovery of Ni and Co from low-grade lateritic nickel ore*. *Materials Today: Proceedings, 30*, 320–324. https://doi.org/10.1016/j.matpr.2020.02.167.
11. Febriana, E., Hidayat, T., Fauzi, I., Irawan, J., Mayangsari, W., Rhamdani, A. R., Prasetyo, A. B., Oediyani, S., & Firdiyono, F. (2026). *Iron removal from acidic limonitic laterite leach solution through controlled oxidative and alkaline precipitation*. *Mining, Metallurgy & Exploration, 43*(3). https://doi.org/10.1007/s42461-026-01548-6.
12. Georgiev, P., Ivanova, M.-F., Nicolova, M., Spasova, I., & Groudev, S. (2020). *Review of the iron recovery processes from laden leach liquors in hydrometallurgy*. *Sustainable Extraction and Processing of Raw Materials, 1*(1), 31–36. https://doi.org/10.58903/a14161825.
13. Hosseini-Nasab, M., Noaparast, M., & Abdollahi, H. (2022). *Selective precipitation of iron from multi-element PLS produced by atmospheric leaching of Ni-Co bearing laterite*. *International Journal of Mining and Geo-Engineering, 56*(2), 309–313. https://doi.org/10.22059/IJMGE.2022.307768.594861.
14. Keber, S., Brückner, L., Elwert, T., & Kuhn, T. (2020). *Concept for a hydrometallurgical processing of a copper-cobalt-nickel alloy made from manganese nodules*. *Chemie Ingenieur Technik, 92*(7), 963–971. https://doi.org/10.1002/cite.201900125.
15. Laubertová, M., Velgosova, O., Sisol, M., & Vindt, T. (2024). *Study of hydrometallurgical treatment of metal-bearing material from environmental burdens containing iron, chromium, nickel, and cobalt*. *Minerals, 14*(10), 968. https://doi.org/10.3390/min14100968.
16. Li, G., Chen, Y., Mang, C., Teng, X., Luo, J., Rao, M., & Hide. (2023). *Near-zero-waste approach for the treatment of saprolitic nickel laterite via a combined hydrometallurgical process*. *ACS Sustainable Chemistry & Engineering, 11*(18), 7246–7258. https://doi.org/10.1021/acssuschemeng.2c05403.
17. Lin, P., & Pan, L. (2024). *Unveiling the mechanism in nickel loss during the neutralization of pregnant acid leach solution by various alkaline chemicals using electron imaging, X-ray diffraction, and electron energy loss spectroscopy analyses*. *Mineral Processing and Extractive Metallurgy Review, 46*(6), 684–700. https://doi.org/10.1080/08827508.2024.2373753.
18. Liu, W., Li, P., Zhang, H., Qin, Q., Wu, F., Zhang, Q., Zheng, S., & Li, G. (2025). *Investigation on the loss of valuable metals during the removal of impurities Fe^{3+} and Al^{3+} from spent lithium-ion battery leaching solutions*. *Inorganic Chemistry Communications, 186*, Article 116115. https://doi.org/10.1016/j.inoche.2025.116115

JIRRS
Journal International Review of Research Studies
Received: 02/05/2026 - **Accepted:** 25/06/2026
Vol: 01.09
DOI: 10.66104/x7rh8151
Pages: 1-39

19. Liu, W., Qin, Q., Zhang, H., Chen, X., Luo, L., Li, G., Zheng, S., & Li, P. (2022). *Novel technology for the removal of Fe and Al from spent Li-ion battery leaching solutions by a precipitation–complexation process*. *ACS Sustainable Chemistry & Engineering, 10*(41), 13605–13615. https://doi.org/10.1021/acssuschemeng.2c03743.
20. Marte, K., & Boone, M. (2025). *Development of the Baptiste Nickel Project—Part 2: Hydrometallurgical refining*. In *Ni-Co 2025: 6th International Symposium on Nickel and Cobalt* (pp. 253–270). Springer Nature Switzerland. https://doi.org/10.1007/978-3-032-00167-2_20.
21. Niu, Z., Li, G., He, D., Fu, X., Sun, W., & Yue, T. (2021). *Resource-recycling and energy-saving innovation for iron removal in hydrometallurgy: Crystal transformation of ferric hydroxide precipitates by hydrothermal treatment*. *Journal of Hazardous Materials, 419*, Article 125972. https://doi.org/10.1016/j.jhazmat.2021.125972.
22. Pereira, A. C. (2026a). *Improving filterability of hydroxide precipitates in hydrometallurgical hydrolysis processes: A critical review*. *IKR Journal of Engineering and Technology (IKRJET), 2*(3). https://doi.org/10.5281/zenodo.20098962.
23. Pereira, A. C. (2026b). *Controlling co-precipitation in hydrometallurgy: From physicochemical parameters to process design and technology readiness*. *IKR Journal of Engineering and Technology (IKRJET), 2*(3). https://doi.org/10.5281/zenodo.20357561
24. Setiawan, I., Oediyani, S., Setiawati, N., Irawan, J., Subagja, R., Rhamdani, A. R., & Lalasari, L. H. (2024). *Iron precipitation from nickel laterite ores using sulfuric acid atmospheric leaching with addition of hydrogen peroxide*. In *Proceedings of the 5th International Seminar on Metallurgy and Materials (ISMM 2022): Strengthening research and innovation in metallurgy and materials for sustainable economic development*. AIP Publishing. https://doi.org/10.1063/5.0186246.
25. Silva, M. F. da, Oliveira, M. R. de S., Santos, I. D. dos, Radino-Rouse, P., Mansur, M. B., & Hide. (2020). Iron precipitation strategies from nickel laterite ore sulfuric acid leach liquor. *Mineral Processing and Extractive Metallurgy Review, 43*(1), 1–12. https://doi.org/10.1080/08827508.2020.1809392.
26. Tayip, D. K., Xu, K., Yang, J., Wan, W., Wardani, A. K., & Chen, Y. (2026). *Sequential purification of manganese-rich leachate from laterite nickel processing residue*. *Journal of Sustainable Metallurgy, 12*(3). https://doi.org/10.1007/s40831-026-01511-1.
27. Wang, W.-W., Liu, C., Qin, B., Liu, Z.-B., Li, X.-Y., Li, M.-C., Liu, G., Lv, D., Lu, Y.-D., Li, J., & Chen, S.-X. (2025). *Comprehensive recovery of valuable metals from laterite via neutralization sludge*. *Separation and Purification Technology, 368*(1–2), Article 133006. https://doi.org/10.1016/j.seppur.2025.133006.
28. Wen, J., Tuan, T. T., & Lee, M.-S. (2024). *Recovery of pure Co(II) and Ni(II) solutions from synthetic sulfate leach liquor of laterite ores by precipitation and solvent extraction*. *Mineral Processing and Extractive Metallurgy Review, 46*(4), 492–501. https://doi.org/10.1080/08827508.2024.2346652.

JIRRS
Journal International Review of Research Studies
Received: 02/05/2026 - **Accepted:** 25/06/2026
Vol: 01.09
DOI: 10.66104/x7rh8151
Pages: 1-39

29. Wijenayake, J. J., Moats, M. S., Mseteka, L. M., & Alagha, L. (2025). *Selective nickel leaching and preparation of battery-grade nickel carbonate from copper-rich industrial intermediate*. *Processes, 13*(10), Article 3235. https://doi.org/10.3390/pr13103235.
30. Xing, Y., Deng, Z., Wei, C., Li, X., & Li, M. (2024). *Transformation behavior of hazardous jarosite into recyclable hematite in a solution with high concentrations of K+ and Na+*. *Scientific Reports, 14*, Article 14086. https://doi.org/10.1038/s41598-024-64755-6.
31. Yang, T., Guo, Z., Wang, M., Zhang, G., Li, Q., Guan, W., Wu, S., & Wu, X. (2025). *Deep removal of sodium and ammonium from nickel sulphate solution by jarosite precipitation method*. *Canadian Metallurgical Quarterly, 65*(1), 1–12. https://doi.org/10.1080/00084433.2025.2500778.
32. Yang, X., Gao, L., Wu, Y., Chen, Y., & Tong, L. (2022). *Extraction of magnesium and nickel from nickel-rich serpentine with sulfation roasting and water leaching*. *Metals, 12*(2), Article 318. https://doi.org/10.3390/met12020318.
33. Yun, S. H., Jang, I. J., & Lee, M.-S. (2025). *Separation of Co(II), Mn(II), and Ni(II) from synthetic sulfuric acid leaching solution of nickel laterite ore by precipitation*. *Mineral Processing and Extractive Metallurgy Review, 46*(8), 1–12. https://doi.org/10.1080/08827508.2025.2565756.
34. Zablotskaya, Y. V., Sadykhov, G. B., Anisonyan, K. G., Smirnova, V. B., & Tuzhilin, A. S. (2022). *On the problem of enhancing selectivity of nickel and cobalt recovery during the sulfuric acid leaching of reduced oxidized nickel ore*. *Russian Metallurgy (Metally), 2022*(9), 985–989. https://doi.org/10.1134/S0036029522090142.
35. Zablotskaya, Y. V., Sadykhov, G. B., Anisonyan, K. G., Smirnova, V. B., & Tuzhilin, A. S. (2023). *Possibility of improving parameters of the sulfuric acid leaching of reduced ferriferrous laterite ores with selective nickel and cobalt recovery*. *Russian Metallurgy (Metally), 2023*(12), 1759–1764. https://doi.org/10.1134/S0036029523120364.
36. Zablotskaya, Y. V., Sadykhov, G. B., Anisonyan, K. G., Tuzhilin, A. S., & Khasanov, M. (2025). *Prospects of the hydrometallurgical processing of laterite nickel ores with selective nickel and cobalt recovery*. *Russian Metallurgy (Metally), 2024*(7), 1544–1549. https://doi.org/10.1134/S0036029524702732.
37. Zhou, X., Chen, Y., Tan, F., An, J., & Yang, W. (2024). Selective removal of iron from sulfuric acid leaching solution of aerospace magnetic material scraps by jarosite process. *Waste Management, 188*, 107–116. https://doi.org/10.1016/j.wasman.2024.08.007.
38. Zhu, Q., Yang, Jg., Nan, Tx. *et al.* Mechanism and application of seed-induced goethite crystal growth for iron removal from rich-zinc solution. *J. Cent. South Univ.* **32**, 837–852 (2025). https://doi.org/10.1007/s11771-024-5774-5.